Plant Physiology Preview. Published on January 24, 2020, as DOI:10.1104/pp.19.01183

**Short title**: Role of plasma membrane aquaporins in maize

**Author for Contact details**: François Chaumont, francois.chaumont@uclouvain.be

# Modification of the expression of the aquaporin ZmPIP2;5 affects water relations and plant growth

Lei Ding,[a,1] Thomas Milhiet,[a,1], Valentin Couvreur,[b] Hilde Nelissen,[c,d] Adel Meziane,[a,e] Boris Parent,[e] Stijn Aesaert,[c,d] Mieke Van Lijsebettens,[c,d] Dirk Inzé,[c,d] François Tardieu,[e] Xavier Draye,[b] François Chaumont[a,2]

[a] Louvain Institute of Biomolecular Science and Technology, UCLouvain, 1348 Louvain-la-Neuve, Belgium

[b] Earth and Life Institute, UCLouvain, 1348 Louvain-la-Neuve, Belgium

[c] Center for Plant Systems Biology, VIB-Ghent University, Technologiepark 71, 9052 Ghent, Belgium

[d] Department of Plant Biotechnology and Bioinformatics, Ghent University, 9052 Gent, Belgium

[e] Laboratoire d'Ecophysiologie des Plantes sous Stress Environnementaux (LEPSE), Université de Montpellier, Institut National de la Recherche Agronomique (INRA), F-34000 Montpellier,

[1]These authors contributed equally to the article.
[2]Author for contact

**One-sentence summary**: Reverse genetic approaches demonstrate that the maize plasma membrane PIP2;5 aquaporin plays a role in controlling root radial water movement, leaf hydraulic conductivity, and plant growth.

**Author contributions**: L.D., T.M., H.N., B.P., and F.C. designed the experiments. L.D., T.M., H.N., A.M., B.P., and S.A. performed the experiments. M.V.L. supervised the maize transformation. L.D., T.M., V.C., H.N., A.M., B.P., S.A., F.T., X.D., M.V.L., and F.C. analyzed the data. L.D. and F.C. wrote the manuscript. All the authors contributed to the discussion and revision of the manuscript.

**Funding information**: This work was supported by the Belgian National Fund for Scientific Research (FNRS, FRFC 2.4.501.06F), the Interuniversity Attraction Poles Programme-Belgian Science Policy (grant IAP7/29), the "Communauté française de Belgique-Actions de Recherches Concertées" (grants ARC11/16-036 and ARC16/21-075) and the Pierre and Colette Bauchau Award. L.D. was supported by an Incoming Post-doc Move-in Louvain Fellowships co-funded by the Marie Curie Actions. T.M. was supported by a research fellow at the Fonds de Formation à la Recherche dans l'Industrie et l'Agriculture.V.C. was supported by the FNRS (FC 84104).

## Abstract

In maize (*Zea mays*), the plasma membrane intrinsic protein PIP2;5 is the most highly expressed aquaporin in roots. Here, we investigated how deregulation of PIP2;5 expression affects water relations and growth using maize overexpressing (OE; B104 inbred) or knockout (KO; W22 inbred) lines. The hydraulic conductivity of the cortex cells of roots grown hydroponically was higher and lower in PIP2;5 OE and *pip2;5* KO lines, respectively, compared with their corresponding wild-type (WT) plants. While whole root conductivity decreased in the KO lines compared to the WT, no difference was observed in OE plants. This paradox was interpreted using the MECHA hydraulic model, which computes the radial flow of water within root sections. The model hints that the plasma membrane permeability of the cells is not radially uniform but PIP2;5 may be saturated in cell layers with apoplastic barriers, i.e. the endodermis and exodermis, suggesting the presence of post-translational mechanisms controlling the abundance of PIP in the plasma membrane in these cells. At the leaf level, where the *PIP2;5* gene is lowly expressed in WT plants, the hydraulic conductance was higher in the PIP2;5 OE lines compared with the WT plants, whereas no difference was observed in the *pip2;5* KO lines. The temporal trend of leaf elongation rate used as a proxy of that of xylem water potential was faster in PIP2;5 OE plants upon mild stress, but not in well-watered condition, demonstrating that PIP2;5 may play a beneficial role for plant growth under specific conditions.

## Introduction

Aquaporins, belonging to the plasma membrane intrinsic protein (PIP) subfamily, are major actors controlling membrane water permeability. The physiological functions of PIPs are straightforward at the cell level (Hachez et al., 2006; Hachez et al., 2008; Hachez et al., 2012; Heinen et al., 2014), but are considerably more complex at the organ and whole-plant levels. For example, overexpression or silencing of PIP aquaporins has contrasting effects on root hydraulics (Siefritz et al., 2002; Hachez et al., 2006; Postaire et al., 2010; Sade et al., 2010), root development (Péret et al., 2012), leaf hydraulic conductance ($K_{leaf}$) (Prado and Maurel, 2013; Sade et al., 2014), stomatal movement (Grondin et al., 2015; Wang et al., 2016; Rodrigues et al., 2017), and transpiration ($T_r$) (Maurel et al., 2016). This is largely because the transcellular path, in which water crosses the cell membranes mainly through aquaporins (Steudle and Peterson, 1998; Steudle, 2000) occurs simultaneously together with other two pathways, namely the apoplastic path, in which water flow goes through the cell wall, and the symplastic path, in which water moves through the plasmodesmata. The overall root hydraulic conductivity ($L_{pr}$) is the integration of conductivity from the three pathways; their contribution to the $L_{pr}$ varies according to root anatomy development and environmental factors (drought, high salinity, nutrient availability, and anoxia, etc.). To better understand the complexity of root radial hydraulic conductivity and integrate the multiple variables, mathematical models have been developed (Steudle and Peterson, 1998; Zwieniecki et al., 2002; Foster and Miklavcic, 2017; Couvreur et al., 2018). Among them, the 'MECHA' model (Couvreur et al., 2018) predicts the root radial hydraulic conductivity, based on the detailed radial anatomy of the root and the distribution of the cell wall hydraulic conductivity, the cell plasma membrane permeability, the hydraulic conductance, the frequency of plasmodesmata, and the membrane reflection coefficients. MECHA is therefore appropriate to address subcellular hydraulics and its impact on the radial transport of water.

Here, we analyzed the effects of the overexpression or silencing of the maize (*Zea mays*) PIP2;5 at both cellular and whole-plant levels. The *PIP2;5* gene encodes an active water channel (Fetter et al., 2004), is the most expressed *PIP* gene in the primary root (Hachez et al., 2006), and shows a polarized localization at the plasma membrane side facing the external medium, supporting a function in root water uptake. Another clue for the involvement of PIP2;5 in radial water movement is its high expression in cell types with Casparian strips (exodermis and endodermis), places where water has to enter the symplast to continue its flow to the xylem vessels (Hachez et al., 2012). In roots, the expression of *PIP2;5* mRNA and its protein abundance are modulated by diurnal and circadian rhythm, osmotic stress, and growth conditions (aeroponic and hydroponic) (Hachez et al., 2012; Caldeira et al., 2014). In addition, PIP2;5 proteins are more or less abundant in maize lines overexpressing or silenced for an ABA biosynthesis gene, respectively (Parent et al., 2009). The *PIP2;5* gene is weakly expressed in leaves, with a maximum of expression at the end of the elongation zone and the zone where the leaf emerges from the sheath and where lignification of the metaxylem is observed (Hachez et al., 2008). Altogether, these data suggest that PIP2;5 plays important roles in regulating water relations in maize, but genetic approaches to further understand its physiological function are missing.

We first characterized PIP2;5 overexpressing (OE) and *pip2;5* knockout (KO) lines at the

molecular and cellular levels and addressed the question of the effects of the manipulation of PIP2;5 expression at the plant level by collectively examining the hydraulic conductance in roots and leaves and the time course of leaf elongation rate, considered here as a way to indirectly assess the changes in xylem water potential, following fluctuations of the evaporative demand (Caldeira et al., 2014; Caldeira et al., 2014). While the cell hydraulic conductivity was affected by the deregulation of PIP2;5 expression, the contrasting results at the organ levels suggest that upscaling requires a modeling approach to decipher the dataset presented here.

## Results

### Generation, Isolation, and Molecular Characterization of Maize Lines Deregulated in PIP2;5 Expression

To determine the role of PIP2;5 aquaporin in maize, we first prepared a genetic construct aiming at constitutively overexpressing the *PIP2;5* gene under the control of the *p35S* promoter (Fig. 1A), and performed an *Agrobacterium*-mediated transformation of the inbred B104. Two independent *PIP2;5* overexpressing lines (PIP2;5 OE-4 and OE-13) with high PIP2;5 protein content from Western blotting analysis (see below) were selected for further molecular characterization. In addition, we obtained from the "Maize Genetic COOP Center" (http://maizecoop.cropsci.uiuc.edu/) a putative *pip2;5* knockout (*pip2;5* KO) W22 inbred line (UFMu00767) containing a *Mu* transposon in the *PIP2;5* gene (Fig. 1B). The presence and the site of insertion of the *Mu* transposon in *PIP2;5* gene were determined by PCR-amplification of genomic DNA using *PIP2;5* and *Mu* specific primers; this showed that the *Mu* transposon was inserted in the second intron of the *PIP2;5* gene (Fig. 1B).

To confirm the overexpression and downregulation of *PIP2;5* in the maize lines, microsomal fractions were prepared from roots and leaves, and PIP2;5 was immunodetected using specific antibodies (Hachez et al., 2006). In roots, where the endogenous *PIP2;5* gene is the highest expressed *PIP* gene, a 17% and 141% increase in PIP2;5 protein abundance in the PIP2;5 OE-4 and OE-13 lines, respectively, were observed when compared with the non-transgenic segregating siblings (B104, named afterwards WT-B104) (Fig. 1C). In leaves, where the endogenous *PIP2;5* is lowly expressed, more than 10-fold higher PIP2;5 protein abundance was detected in the PIP2;5 OE-4 and OE-13 lines compared with the WT-B104 plants (Fig. 1D). On the other hand, the PIP2;5 protein level was ninefold lower in the roots of *pip2;5* KO line than in roots of non-transgenic segregating siblings (W22, named afterwards WT-W22) (Fig. 1C). No significant difference in PIP2;5 signal intensity was found between *pip2;5* KO and WT-W22 leaves (Fig. 1D), but the PIP2;5 signals in leaves were hardly detectable and only observed after a very long exposure.

We also analyzed the *PIP2;5* mRNA levels in roots and leaves by RT-qPCR. In the OE plants, while no difference in *PIP2;5* endogenous mRNA levels were observed, a high *PIP2;5* transgene mRNA signal was detected using a *PIP2;5*-specific forward primer and a construct linker-specific reverse primer (Supplemental Fig. S1, A-D). No amplification was detected with this pair of primers in the WT-B104 plants. In *pip2;5* KO plants, we observed 2175-fold and fivefold lower mRNA level in roots (Supplemental Fig. S1E) and leaves (Supplemental Fig. S1F), respectively, than in the WT-W22 plants. To investigate the reason why a very faint protein signal was still observed in the leaf extract by immunodetection, we performed

RT-qPCR with primers flanking the Mu insertion site and detected a weak signal (Supplemental Fig. S2), suggesting that the *pip2;5* KO plants are not a complete loss-of-function line.

To investigate whether the expression of other PIPs was affected by the deregulation of *PIP2;5* gene in both roots and leaves, RT-qPCR and Western blotting were performed. No significant difference in the mRNA levels of most *PIPs* was observed between PIP2;5 OE lines or *pip2;5* KO and their corresponding WT lines in both roots and leaves (Supplemental Fig. S1). Similarly, at the protein level, no significant difference in PIP1;2 and PIP2;1/2;2 was observed between the OE or KO lines and their respective WT plants (Supplemental Fig. S3).

Because we used two different maize genetic backgrounds in this work, we checked that the expression pattern of PIP2;5 was similar in the W22 and B73 lines (Hachez et al., 2006, 2008 and 2012). Similar to the previous results obtained in the B73, an intense signal of PIP2;5 was immunodetected in the exo- and endodermis cells of W22 root, where the lignin and suberin are deposited (Supplemental Fig. S4, A and B). *PIP2;5* was also the most highly expressed *PIP* gene in W22 roots and was lowly expressed in leaves (Supplemental Fig. S4C).

**Altered Hydraulic Conductance in the PIP2;5 Deregulated Plants**

We first investigated the effect of PIP2;5 deregulation on the hydraulic conductivity of the root cortex cell ($L_{pc}$), measured with a cell pressure probe. The half-time of water exchange ($T_{1/2}$) across the membrane of root cortex cells was 1.9 to 1.8 times shorter (faster water flow) in the two PIP2;5 OE lines than in WT-B104, whereas $T_{1/2}$ was 2.8 times longer (slower water flow) in the *pip2;5* KO line with respect to the WT-W22 (Table 1). As a result, the $L_{pc}$ was 69% and 67% higher in PIP2;5 OE-4 and OE-13 lines, respectively (Fig. 2, A and B). In contrast, the $L_{pc}$ decreased by 63% in the *pip2;5* KO line compared with the WT-W22 (Fig. 2C). The turgor pressure and the cell elastic modulus ($\varepsilon$) were not affected by the deregulation of PIP2;5 expression (Table 1), with the exception of a higher $\varepsilon_{corrected}$ in PIP2;5 OE-13 lines than in WT-B104 plants. Besides, a bigger cell volume was also measured in PIP2;5 OE-13 lines than in WT-B104 plants, suggesting that PIP2;5 overexpression in this line has affected the root cell expansion. Consistently, the membrane water permeability of leaf mesophyll protoplasts ($P_{os}$) was significantly higher in both PIP2;5 OE lines than in WT-B104 plants (Fig. 2, D and E). In comparison with WT-B104, an 85% and 60% increase in $P_{os}$ was observed in PIP2;5 OE-4 and PIP2;5 OE-13 lines, respectively. On the other hand, no difference in $P_{os}$ was observed between the WT-W22 and *pip2;5* KO lines (Fig. 2F), due to the fact that *PIP2;5* is barely expressed in WT leaves. It is worth mentioning that the $L_{pc}$ and $P_{os}$ mean values were higher in WT-W22 than in WT-B104, suggesting that both inbred lines have different intrinsic membrane permeabilities.

Consistent with the results at the cell level, the leaf hydraulic conductance ($K_{leaf}$) measured with a hydraulic conductance flow meter (HCFM), increased by 58 % and 171 % in the PIP2;5 OE-4 and OE-13 lines, respectively, when compared with the $K_{leaf}$ of WT-B104 plants (Fig. 3, D and E), whereas no significant difference in $K_{leaf}$ was found between *pip2;5* KO plants and WT-W22 plants (Fig. 3F). However, at the root level, the increase in $L_{pc}$ did not result in a significant difference in the whole root conductance ($L_{pr}$) between the WT-B104 and the PIP2;5 OE lines (Fig. 3, A and B). Conversely, $L_{pr}$ was significantly lower in the *pip2;5* KO line than in the WT-W22 (Fig. 3C).

The lack of correlation between cortex $L_{pc}$ and $L_{pr}$ in PIP2;5 OE plants is not a straightforward result to decipher. There are two reasons for this: (1) There are multiple hydraulic media in series across the root radius (including cell walls, membranes, and plasmodesmata, whose hydraulic conductivity may vary in each cell layer). $L_{pr}$ is mostly sensitive to the hydraulic conductivity of media that limit water flow the most (e.g. at gatekeeper cell layers, i.e. endodermis and exodermis, where water flow through cell walls is limited by apoplastic barriers). (2) Root hydraulic media are arranged both in series and parallel, so that water pathways may bypass some of the most limiting media (e.g. at gatekeeper cells, water may bypass cell walls by flowing through membranes, and a fraction of water flow also bypasses gatekeeper cell membranes by using a symplastic path). Hence, the quantitative modeling tool MECHA (Couvreur et al., 2018) with subcellular resolution of water flow was needed to statistically validate the significance of hypotheses possibly explaining the lack of correlation between cortex $L_{pc}$ and $L_{pr}$ between WT and PIP2;5 OE plants. Hypothesis A considered that plasma membrane $L_{pc}$ is uniform across cell layers (Fig. 4A), while hypothesis B considered that PIP2;5 is already "saturated" in WT gatekeeper cells (their $L_{pc}$ equals that measured in the cortex of PIP2;5 OE lines) and "unsaturated" in other cell layers (their $L_{pc}$ equals that measured in the WT cortex) (Fig. 4E). Three values of cell wall hydraulic conductivity ($k_{w\ 1\text{-}3}$), spanning a range from the literature, were considered for each hypothesis. Statistical analysis of results from this combined modeling and experimental approach suggested that, given the observed $L_{pc}$ in WT-B104 and PIP2;5 OE plants, radially uniform patterns of cell membrane permeability may not account for the observed contrast between $L_{pr}$ in WT-B104 and PIP2;5 OE-4 line, regardless of the cell wall hydraulic conductivity $k_w$ (Fig. 4C, $p < 0.01$). The simulations reproduced the observed contrasts between PIP2;5 OE and KO lines (Fig. 4, F-H) at the conditions that $k_w$ was higher than $6.9\times10^{-10}$ $m^2.s^{-1}.MPa^{-1}$ ($k_{w2}$), and that the contribution of PIP2;5 to $L_{pc}$ was saturated in the endodermis and exodermis of WT lines (Fig. 4E, $p < 0.05$).

**Altered Plant Growth in PIP2;5 Deregulated Plants Under Water Deficit Conditions**

To further investigate the effect of PIP2;5 deregulation on water relations and plant growth, we examined the time course of leaf elongation rate (LER) over changes in environmental conditions. During the day, while the evaporative demand increases, hydraulic resistances to water transfer can rapidly decrease the leaf water potential ($\Psi_{leaf}$) and the leaf growth, but it is only observable under suboptimal water conditions (Bouchabké et al., 2006). We therefore measured the leaf water potential and expansion of PIP2;5 OE-4 plants and their WT-B104 under well-watered conditions (Fig. 5C, in order to observe putative intrinsic differences of leaf expansion rate) and under moderate water deficit (Fig. 5D, in order to observe the effects of hydraulics).

Under moderate water deficit ($\Psi_{soil}$ = -0.23 to -0.26 MPa), we measured a higher leaf water potential in the PIP2;5 OE-4 line than in WT-B104 plants, while the difference was not observed under well-watered conditions (Fig. 5B). A significantly faster recovery of LER was observed after the early-morning drop in PIP2;5 OE-4 compared with WT-B104 plants resulting in large differences of LER during the day (Fig. 5D, inset). Overall, the mean LER of PIP2;5 was higher in OE-4 than in WT-B104 over one day (Supplemental Fig. S5, 0.75 $mm.h^{-1}$ vs 0.40 $mm.h^{-1}$). During the night, the average LER of PIP2;5 OE-4 was 1.42 $mm.h^{-1}$

and it was also significantly higher ($p < 0.001$) than the average LER of WT-B104 (1.05 $mm.h^{-1}$). As expected, these differences were not observed in well-watered conditions (Fig. 5C), indicating that no pleiotropic effects had affected the intrinsic potential leaf expansion rate of OE plants.

A faster recovery of LER was correlated with an increase in PIP aquaporin expression, $\Psi_{leaf}$ and $L_{pr}$ (Parent et al., 2009; Caldeira et al., 2014). While no change in $L_{pr}$ was recorded in PIP2;5 OE plants compared with the WT-B104 plants in well-watered condition, we compared the $L_{pr}$ in response to short term osmotic stress (10% w/v polyethylene glycol (PEG) 6000; $\Psi$ = -0.15 MPa) and observed a higher $L_{pr}$, but not significantly different, in PIP2;5 OE-4 than in WT-B104 plants (Supplemental Fig. S6). These results suggest that the higher root hydraulic conductivity for PIP2;5 OE-4 observed under low osmotic potential translated into differences of leaf water potential and leaf expansion under moderate water deficit, which was not the case under well-watered conditions due to the very low difference of root hydraulic conductivity.

## Discussion

A better understanding of the functional role of PIP aquaporins in plant water relations is essential to develop crop lines that use water more efficiently and are more tolerant to water deficit. To this aim, we investigated the direct contribution of PIP2;5, the most expressed PIP aquaporin in maize roots, using reverse genetic approaches. Overexpression of *PIP2;5* under the control of the 35S promoter led to a less than two-fold increase in the PIP2;5 protein level in roots, where PIP2;5 is already highly expressed, and an approximately 10-fold increase in leaves, where PIP2;5 is lowly expressed. This difference in PIP2;5 protein abundance according to the organ suggests the existence of post-transcriptional or post-translational regulation mechanisms that prevent an excess of PIP2;5 proteins according to the cell type. Different cellular mechanisms modifying PIP abundance in the plasma membrane have been reported (Chaumont and Tyerman, 2014; Maurel et al., 2015), and involve internalization of PIPs from the plasma membrane for their degradation and/or recycling. Negative feedback of *PIP* gene transcription could not be excluded either, even though it was not detected by RT-qPCR. The decrease in *PIP2;5* gene expression was obtained using the UniformMu transposon mutated line UFMu00767 (McCarty et al., 2005; McCarty et al., 2013; Hunter et al., 2014). In this line, the transposon was inserted in the second intron leading to an important decrease in mRNA and protein levels. However, a very weak signal for PIP2;5 protein was still observed in roots, indicating that the line was not a complete knockout as demonstrated by RT-qPCR using primers flanking the Mu insertion site allowing the detection of a weak signal in *pip2;5* KO samples (Supplemental Fig. S2).

The cortex cell $L_{pc}$ in intact roots was dependent on PIP2;5 expression levels, with higher and lower values in OE and KO lines, respectively. As no change in the abundance of other PIP aquaporins was detected, this is a direct evidence that PIP2;5 facilitated the water diffusion through the cell membranes. We previously showed a correlation between PIP expression and the $L_{pc}$ in roots. The higher abundance of PIPs, including PIP2;5, during the day than during the night, or after a short (8 h) PEG treatment is correlated with variation in the $L_{pc}$ values (Hachez et al., 2012). Overexpression or knocking out *PIP* genes in other plant

species also results in higher or lower $L_{pc}$. For instance, in *Arabidopsis thaliana pip2;2* KO lines, $L_{pc}$ of the root cortex cells is reduced by ~25% when compared with WT plants (Javot et al., 2003). In contrast, $L_{pc}$ is higher in PIP2;5 overexpressing Arabidopsis lines than in WT under low temperature (Lee et al., 2012).

While the $L_{pr}$ of *pip2;5* KO plants was significantly decreased, no increase in $L_{pr}$ was recorded in PIP2;5 OE plants under well-watered conditions, indicating that the abundance of PIP2;5 in the root cell membranes is not always correlated to the $L_{pr}$. The uncorrelated data between PIP abundance, $L_{pc}$, and $L_{pr}$ was previously observed in maize plants subjected to a short PEG stress, which induces a higher PIP expression and a higher $L_{pc}$, but no change in $L_{pr}$ (Hachez et al., 2012). The composite water transport model (Steudle and Peterson, 1998) assumes that $L_{pr}$ is controlled by the hydraulic conductivity of apoplastic and cell-to-cell pathways in parallel. We proposed that radial variations along each pathway critically affect water transport due to the presence of gatekeeper cells at the beginning (epidermis and exodermis) or the end (endodermis) of the radial path of water (Hachez et al., 2012; Chaumont and Tyerman, 2014). While the current cell pressure probe technology did not allow to directly verify this hypothesis, the use of the quantitative modeling framework MECHA (Couvreur et al., 2018) gave us the opportunity to get a better understanding of the mechanisms involved. The statistical comparison of our measured and simulated $L_{pr}$ results largely supports the hypothesis that plasma membrane permeability is not radially uniform in WT (hypothesis A rejected, $p < 0.01$, Fig. 4C) but may be saturated in the endodermis and exodermis (hypothesis B, Fig. 4E), thus following the observed radial aquaporin expression patterns observed by Hachez et al. (2006). This is an important result, as none of the simplest to most sophisticated models of radial water flow account for such heterogeneity, which does affect $L_{pr}$ in WT. On the other hand, knocking-out *PIP2;5* gene expression led to a decrease in $L_{pr}$ suggesting that PIP2;5 is an essential actor facilitating radial water flow and controlling whole root conductivity, as also observed in our simulations. Quantification of the level of active PIP2;5 proteins in the endodermis would be very informative. Indeed, *PIP2;5* gene overexpression in this specific cell type would not lead to an increase in PIP2;5 protein due to the above-mentioned post-translational mechanisms and that a maximum of active PIP2;5 (and other PIPs) was already reached. These predictions could be refined by generating maize lines with deregulated PIP expression exclusively in the endodermis or the exodermis.

Maize lines expressing *PIP2;5* cDNA under the control of *p35*S promoter showed a much higher increase in PIP2;5 protein abundance in leaves than in roots. Considering that general PIP expression in maize leaves is lower than in roots and that *PIP2;5* is very lowly expressed in leaves (Hachez et al., 2006; Hachez et al., 2008; Heinen et al., 2009), we hypothesize that overexpressing PIP2;5 in this organ was not limited by similar post-transcriptional or post-translational mechanisms observed in roots. Similar to what was observed in root cells, an increase in $P_{os}$ was measured for the leaf mesophyll cells overexpressing PIP2;5. We previously demonstrated that transient expression of PIP2;5 in mesophyll cells increases the water membrane permeability (Besserer et al., 2012). But in contrast to the effect of PIP2;5OE on the whole root conductance, overexpression of PIP2;5 led to a higher $K_{leaf}$ compared to the $K_{leaf}$ of WT-B104 plants (Fig. 3, D and E). A similar result was found, for instance, in tomato plants overexpressing NtAQP1 (Sade et al., 2010). Inversely, downregulation of *PIP1* gene expression in Arabidopsis plants results in a decrease in the

mesophyll cell $P_{os}$ and the $K_{leaf}$ (Sade et al., 2014). $K_{leaf}$ and the leaf radial water flow are thought to be mainly controlled by the vascular bundle sheath cells surrounding the veins (Sack and Holbrook, 2006; Shatil-Cohen et al., 2011; Buckley, 2015). These cells can have suberized walls, and are associated with a very low apoplastic flow. Arabidopsis plants, in which *PIP1* genes are specifically silenced in these cells, also exhibit decreased mesophyll and bundle sheath $P_{os}$ and decreased $K_{leaf}$ (Sade et al., 2014). In our work, PIP2;5 OE plants exhibited higher $P_{os}$ of the mesophyll cells and possibly also of the bundle sheath cells, resulting in an enhancement of conductance in bundle sheath, mesophyll cells, and $K_{leaf}$. The observation that no difference in $P_{os}$ and $K_{leaf}$ was observed in *pip2;5* KO plants was expected since PIP2;5 is lowly expressed in leaf tissues (Hachez et al., 2008). Extending the MECHA model to leaf tissues and cells will be very useful to address these questions related to leaf water relations.

LER is controlled by plant hydraulic properties, including leaf and xylem water potential, transpiration and root hydraulic conductivity (Caldeira et al., 2014), and involved hormonal regulation (Nelissen et al., 2012; Avramova et al., 2015; Nelissen et al., 2018). Actually, we considered that short-term variation of LER is a proxy of the change of xylem water potential (Parent et al; 2009; Caldeira et al., 2014a). In a mild water deficit, a faster recovery of LER after the early morning drop was recorded in PIP2;5 OE-4 compared with WT-B104 plants, and a higher LER during the day and night was recorded. This LER response in PIP2;5 OE plants can be correlated with a higher $K_{leaf}$ and is consistent with the effect of $K_{leaf}$ on LER recovery observed in transgenic plants that differ in ABA concentration in the xylem sap, showing differences in $L_{pr}$ (Parent et al., 2009). Interestingly, while WT-B104 and PIP2;5 OE plants had a similar $L_{pr}$ in well-watered conditions, an osmotic stress led to an increased $L_{pr}$ in the OE plants, suggesting that changes in hydraulic conductance ($L_{pr}$ and $K_{leaf}$) by PIP2;5 deregulation at the cell level translated into an overall change in whole plant hydraulic fluxes (and leaf water potential) that affects the LER in mild-stress conditions. The observation that the LER was not affected in well-watered plants implies that molecular mechanisms controlling the overall root hydraulic conductance occur in some cell types resulting in a non-uniform distribution of water permeability (see above) or at specific positions along the root axis (e.g. the connection between root and leaf xylems).

In conclusion, deregulation of PIP2;5 aquaporin expression in maize plants highlighted their role in controlling the root and leaf cell water permeability. However, understanding the results obtained at the root level has required a hydraulic model developed at the cell and tissue scales. MECHA allowed us to discard the hypothesis of radially uniform $L_{pc}$, and suggests that, in well-watered conditions, the gatekeeper cells of WT plants have a saturated membrane permeability. Transposing the model to the aerial part will definitely offer possibilities to better understand the hydraulic properties of tissues and cells in diverse conditions and investigate the role and regulation of aquaporins in specific hydraulic processes. Indeed, we showed that the increase in the hydraulic conductance by overexpressing aquaporin positively affects the LER under moderate stress conditions.

## Materials and Methods

**Plasmids and genetic construction to generate PIP2;5 overexpressing lines**

The cauliflower mosaic virus *p35S* promoter was PCR-amplified from the pMDC43 vector (Curtis and Grossniklaus, 2003) and cloned into the Gateway entry vector pDONR P4-P1R (Invitrogen, Carlsbad, US) following the manufacturer's instructions. The *YFP* cDNA followed by the *tnos* terminator sequence was amplified together from the pH35GY vector (Kubo et al., 2005) and cloned into the pDONR221 vector. Finally, a uracil-excision based cloning cassette (USER) was added downstream of the *p35S* promoter sequence and subsequently cloned into pDONR P2R-P3 (Nour-Eldin et al., 2006; Hebelstrup et al., 2010). These three entry vectors were verified by sequencing and their inserts brought together by LR recombination into the pBb7m34GW backbone vector suitable for maize (*Zea mays*) transformation (Karimi et al., 2013) (https://gateway.psb.ugent.be). The latter contains the *bar* selectable gene under the control of the *p35S* promoter that induces resistance to the herbicide bialaphos and allows selecting transformed calli and shoots using phosphinotricin-containing media. The cDNA encoding ZmPIP2;5 was PCR-amplified using USER primers (forward primer: 5' GGTCTTAAUATGGCCAAGGACATCGAGG 3'; reverse primer: 5' GGCATTAAUCTAGCGGCTGAAGGAGGCA 3') and inserted into the destination vector to obtain the final vector. This plasmid was used to transform the hypervirulent EHA101 *Agrobacterium tumefaciens* strain (Hood et al., 1986) by heat shock and subsequently used for transformation of maize immature embryos from B104 inbred line according to the method described by Coussens et al. (2012), in collaboration with the Maize Transformation platform of the Center Plant Systems Biology (VIB-Ghent University, Belgium). Briefly, immature embryos were isolated from the ears 12 to 14 days after fertilization and co-cultivated with EHA101 *A. tumefaciens* strain carrying the plasmid of interest for three days in the dark at 21℃. After co-cultivation, immature embryos were cultivated for one week without selection, followed by a four-month period of subculturing on selective media containing increasing amounts of phosphinotricin (starting from 1.5 mg/l to 6 mg/l) to select transformed embryogenic calli in dark conditions at 25℃. After selection, the embryogenic calli were transferred to bigger containers and placed in a growth chamber (24℃, 55µE.$m^{-2}$.$s^{-1}$ light intensity, 16h/8h day/night regime) for transgenic T0 shoot/plantlet formation *in vitro*. Eleven rooted transgenic T0 plants selected from independently transformed immature embryos tested positive for the phosphinotricin acetyltransferase (PAT) enzyme (encoded by the *bar* selectable marker gene) using the TraitChek Crop and Grain Test Kit (Strategic Diagnostics, Newark, DE, USA. The presence of the transgenic *ZmPIP2;5* cDNA insertion was also confirmed by PCR amplification of genomic DNA using *p35S* forward primer (5' CCACTATCCTTCGCAAGACCC 3') and *T35S* reverse primer (5' GGTGATTTTTGCGGACTCTAGCAT 3'). The transgenic T0 plants were transferred to soil and kept one month in a growth chamber (16h/8h day/night regime at 24 ℃, 55 µmol.$m^{-2}$.$s^{-1}$ light intensity, and 55% relative humidity) in 1 L pots for acclimation, and then moved to a greenhouse (26 ℃/22 ℃, day/night temperature, 300 µmol.$m^{-2}$.$s^{-1}$ light intensity under 16h/8h day/night regime) in 10 L pots until flowering. A backcross with the B104 genotype was performed by either pollinating ears of T0 plants with B104 pollen, or pollinating B104 ears with T0 plants pollen. The ears were then harvested 4 weeks after fertilization and dried for several weeks at 25℃ before sowing the segregating T1 generation. The T2 generation

was generated by backcross between B104 and the heterozygous T1 plant in the greenhouse. T1 and T2 generation heterozygous plants segregating for the *ZmPIP2;5* transgene (PIP2;5 OE) and non-transgenic siblings (WT-B104) were used in this study. Finally, two independent overexpressing lines (PIP2;5 OE-4 and PIP2;5 OE-13) with high ZmPIP2;5 protein content in Western blotting analysis were used for all further measurements.

### *pip2;5* KO line

The *pip2;5* KO line (UFMu00767, generated from the W22 inbred line, was found in MaizeGDB (https://maizegdb.org/) and obtained from Uniform Mu stocks in "Maize Genetic COOP Center" (http://maizecoop.cropsci.uiuc.edu/). To confirm the Mu transposon insertion in *PIP2;5* gene, gDNA was extracted from the second leaf of one-week old maize seedling, with the extraction buffer TPS (100 mM Tris-HCl, pH 8.0, 10 mM EDTA, 1 M KCl). PCR was performed using a Mu-TIR specific forward primer (McCarty et al., 2013) (Mu-Terminal Inverted Repeat, TIR6: 5` AGAGAAGCCAACGCCAWCGCCTCYATTTCGTC 3`) and *PIP2;5* specific reverse primer (5` CGTCTACACCGTCTTCTCCG 3`) to detect the Mu insertion, and with *PIP2;5* specific primers (Forward: 5` AGGCAGACGATCCCAGCTT 3`, Reverse: 5` CGTCTACACCGTCTTCTCCG 3`) to detect the *PIP2;5* gene. Heterozygous plants were self-pollinated and a segregation ratio of 1:2:1 for WT-W22, heterozygous, and homozygous seeds was obtained. The WT-W22 and homozygous plants were used for the measurements.

### Growth conditions

Hydroponic culturing was conducted to obtain plant material for the measurements of the cell hydraulic conductivity, root hydraulic conductivity, and leaf hydraulic conductance. Maize seeds were surface sterilized using 2% (w/v) NaClO solution for 5 min, rinsed with distilled water, and placed between two wet tissue papers in a square Petri dish (Greiner Bio-One, Vilvoorde, Belgium). The seeds were put in the dark at 30℃ for 72 h. After germination, the seedlings were transferred to a 2 L beaker with 1/2 strength nutrient solution (1.43 mM $Ca(NO_3)_2.4H_2O$, 0.32 mM $KH_2PO_4$, 0.35 mM $K_2SO_4$, 1.65 mM $MgSO_4.7H_2O$, 9.1 μM $MnCl_2.4H_2O$, 0.52 μM $(NH_4)_6Mo_7O_{24}.4H_2O$, 18.5 μM $H_3BO_3$, 0.15 μM $ZnSO_4.7H_2O$, 0.16 μM $CuSO_4.5H_2O$, and 35.8 μM Fe-EDTA. The nutrient solution pH was adjusted to 5.5 and replaced every two days. The nutrient solution was aerated with the aid of aquarium diffusers. After one week, the full-strength nutrient solution was used until the end of experiments. The plants were grown in a growth chamber at a 16h/8 h light/dark cycle (25/18℃) and a daytime light intensity of 200 $\mu mol.m^{-2}.s^{-1}$ at the top of the leaf level.

Soil culturing was conducted in the growth chamber or in the greenhouse. Maize seeds were surface sterilized using 2% (w/v) NaClO solution for 5 min, rinsed with distilled water, and placed in Jiffypots® (6 cm diameter), filled with 80% potting soil (DCM, Grobbendonk, Belgium) and 20% vermiculite (Agra-vermiculite, Pull Rhenen, Netherland). After two weeks, the seedlings were transferred to a 2 L pots (MCl 17, Pöppelmann, Geluwe, Belgium) filled with the same substrate and vermiculite. After another 4 weeks, the plants were transferred to a 10 L pot (MCl 29).

### Protein extraction and Western blot

Microsomal membrane fractions were prepared as described by Hachez et al. (2006) with a few modifications. Briefly, leaf (newly expanded leaf) or root (primary root) tissues from one-week old maize seedling were flash-frozen in liquid nitrogen in aluminum foil and grinded with mortar and pestle using 2 ml of extraction buffer (250 mM sorbitol, 50 mM Tris-HCl pH 8, 2 mM EDTA,) containing freshly added 0.6% (w/v) polyvinyl pyrrolidone K30, 1 mM phenylmethanesulfonate, 0.5 mM dithiothreitol, and supplemented with 2 $\mu g.ml^{-1}$ of protease inhibitors (leupeptin, aprotinin, antipain, pepstatin, and chymostatin). Debris were removed with a first centrifugation at 770*g* at 4℃ for 10 min and the subsequent supernatant was centrifuged at 10,000*g* at 4℃ for 10 min. The supernatant was then centrifuged at 54,000*g* at 4℃ for 30 min and the resulting pellet (microsomal fraction) was resuspended in 50 µl of suspension buffer (330 mM sucrose, 5 mM $KH_2PO_4$, 3 mM KCl, pH 7.8) and sonicated twice for 5 s. Total protein concentration was determined by the Bradford protein assay (Bradford, 1976).

Twenty µg (for root) and 30 µg (for leaf) of total proteins were mixed with 6X Laemmli buffer (240 mM Tris-HCl, pH 6.8, 6% w/v SDS, 30% w/v glycerol, 0.05% w/v bromophenol blue) and freshly added 10% w/v dithiothreitol, in a total volume of 45 µl. They were solubilized for 10 min at 60℃ were loaded in 12% acrylamide gels (Eurogentec, Seraing, Belgium) for separation by electrophoresis (120V, ~1h). After transfer to a polyvinylidene fluoride membrane (Trans-Blot® Turbo™ Mini PVDF Transfer Packs, Biorad, CA, USA), the proteins were immunodetected using antisera raised against the amino-terminal peptides of ZmPIP1;2, ZmPIP2;1/2;2, and ZmPIP2;5 (Hachez et al., 2006; Hachez et al., 2012). The antibody raised against $H^+$-ATPase (PMA) (Morsomme et al., 1996) was used as control to normalize the protein level. The blotting signal was detected using an Amersham imager 600 (GE Healthcare, Chicago, USA). The signal was quantified with ImageJ software (National Institutes of Health, http://rsb.info.nih.gov/ij) and normalized with the signal of PMA.

**RNA extraction and reverse transcription quantitative PCR (RT-qPCR)**

One-week old maize seedlings were used for RNA extraction and RT-qPCR. The whole newly expanded leaf and primary root were harvested and immediately frozen in liquid nitrogen, and the samples were stored at -80℃ until RNA extraction. RNA extraction was performed with the Spectrum™ Plant Total RNA Kit (Sigma-Aldrich, Mo, US) according to the manufacturer's instructions. DNAse I (Sigma-Aldrich) digestion was performed directly on the column during RNA extraction according to the manufacturer's recommendations. The RNA concentrations and the quality of each sample were measured with a Nanodrop ND-1000 (Isogen Life Science, Utrecht, Netherland), and 1.5 µg of total RNA was used for reverse transcription and the cDNA synthesis was performed with the Moloney Murine Leukemia Virus Reverse Transcriptase (M-MLV RT) kit (Promega, Leiden, Netherland) according to the manufacturer's instructions. RT-qPCR was performed in 96-well plates using a StepOnePlus™ Real-Time PCR System (Life Technologies, Foster City, CA, USA) in a volume of 20 µl containing 10 µl of RT-qPCR Mastermix Plus for SYBR Green I (Eurogentec, Liège, Belgium), 1 µl of forward and reverse primers (Supplemental Table S1), 1 µl cDNA, and 7 µl DEPC-$H_2O$. The PCR cycle program was 2 min at 50℃, 10 min at 95℃ for DNA polymerase activation, and 40 cycles of 15 s at 95℃ and 60 s at 60℃. The $2^{-\Delta Ct}$ method was used to analyze the relative expression of 6 *ZmPIP1s* (*ZmPIP1;1*, *ZmPIP1;2*, *ZmPIP1;3*,

*ZmPIP1;4*, *ZmPIP1;5*, and *ZmPIP1;6*) and 6 *ZmPIP2s* (*ZmPIP2;1*, *ZmPIP2;2*, *ZmPIP2;3*, *ZmPIP2;4*, *ZmPIP2;5*, and *ZmPIP2;6*). Three reference genes, *ACT1*, *EF1-α*, and *polyubiquitin* were used to normalize the expression.

**Cell pressure probe measurement**

One-week old maize seedlings were used for cell pressure probe measurements, according to Hachez et al. (2012) and Volkov et al. (2006). Briefly, the plant and primary root was maintained in a Petri dish containing the nutrient solution and the root region near to the last lateral root (5-7 cm near the root tip) was measured. Cell turgor pressure (P), $T_{1/2}$ (half-time of water across cell membrane), and pressure change value ($\Delta P$) were recorded. These parameters for three to five cells from each plant were measured and three to five plants were analyzed. After the measurements, average values of cell volume and cell surface area were calculated through microscopic analyses of 7-30 cells from the 3$^{rd}$ to 6$^{th}$ cell layer taken at 5-7 cm from the root tip. Cell osmotic pressure was checked with micro-osmometer (Advanced, model 3300, Norwood, Massachusetts, USA). In this study, a cell osmotic pressure of 0.88 MPa was used for all calculations. Cell elastic modulus ($\varepsilon$) and cell hydraulic conductivity ($L_{pc}$) were calculated according to Volkov et al. (2006).

**Root hydraulic conductivity ($L_{pr}$) and leaf hydraulic conductance ($K_{leaf}$) measurement**

Three-week old maize plants growing in phytotron were used for root hydraulic conductivity ($L_{pr}$) measurements, according to Ding et al. (2015). In the phytotron, the light cycling was from 06:00 to 22:00. In the morning between 09:00~11:00 (measurements beginning three hours after light onset), the primary root was cut and connected to a hydraulic conductance flow meter (HCFM, Decagon Devices, Pillman, WA, USA). The connection was performed as quickly as possible (< 1 or 2 min) to minimize the effect of the root excision on the $L_{pr}$ as previously reported by Vandeleur et al. (2014). Transient method was used to recording the value change of flow rate (F) and applied pressure (Pi), and the slope rate (Kr, $Kg.s^{-1}.MPa^{-1}$) was analyzed between the correlation of F and Pi. For one root, three to five replications were performed for the measurement. After the measurement, the primary root was scanned with Epson perfection V33 scanner (EPSON, Japan) and the root surface area was analyzed with ImageJ (National Institutes of Health, http://rsb.info.nih.gov/ij). Then the Kr was normalized with the root surface area for the $L_{pr}$ calculation. For PEG treated plants, 10% (w/v) PEG-6000 was added to the nutrient solution in hydroponic culture, and $L_{pr}$ was measured after 2- and 4-h.

Leaf hydraulic conductance ($K_{leaf}$) was measured between 13:00~15:00 (measurements beginning seven hours after light onset) with HCFM (Tyree et al., 2004; Ferrio et al., 2012) using three-week old maize plants. The newly expanded leaf was cut with the leaf sheath, and coated surrounding a plastic stick covered by UHU®patafix (UHU, Baden, Germany). Then a tape of polytetrafluoroethylene film was wrapped around the leaf sheath. After, the leaf sheath was excised under water and connected with the HCFM. Approximately 0.2 MPa pressure was applied in the system and quasi-steady state method was used to record the flow rate and conductance by every 8 s during 10-30min until the conductance was constant. During the measurement, the leaf was immersed in water to stop transpiration. After the measurement, the leaf was scanned with Epson perfection V33 scanner (EPSON, Japan) and leaf area was

analyzed with ImageJ software. The hydraulic conductance was normalized with the leaf area to calculate the $K_{leaf}$.

**Protoplast swelling assay**

Leaf mesophyll protoplasts were isolated from newly expanded leaves of three-week old maize plants, and swelling assay was performed according to Moshelion et al. (2004) and Shatil-Cohen et al. (2014). The leaf abaxial side was scratched with a glass-paper, and then the leaf was cut into small sections and transferred to the digestion buffer (the scratched side contact with the buffer), including 0.6% (w/v) cellulose R10 (Duchefa Biochemine, Haarlem, Netherland), 0.1% (w/v) pectolyase (Sigma-Aldrich, Mo, US), 0.3% (w/v) Macerozyme R10 (Duchefa Biochemine, Haarlem, NL), 5 $mg.ml^{-1}$ bovine serum albumin, and 5 $mg.ml^{-1}$ polyvinyl pyrrolidone K30. The analysis of the osmotic water permeability coefficient was according to Shatil-Cohen et al. (2014).

**Leaf elongation rate measurement**

Leaf growth was measured in the high throughput phenotyping platform Phenodyn (Sadok et al., 2007) of the LEPSE laboratory in Montpellier (https://www6.montpellier.inra.fr/*lepse*/*M3P*). Plants were grown in one PVC column, filled with clay balls, which allows to tare columns at 1.2 kg. Then, columns were filled with 4.4 kg of a mix of loam (5-10%) and soil. Plants were daily watered with nutritive solution. Sampling of the newest leaf was carried out at 4-leaf stage and a PCR was made in order to characterize the transgenic PIP2;5 OE plants. After the characterization, three plants were kept in the column, including either three WT-B104 or PIP2;5 OE plants or a mix of them (either two WT-B104 or two PIP2;5 OE) for the LER measurement. Plants were grown under a 14 h light / 10 h dark cycle at 19-26℃ (day, mini-maxi)/19-21℃ (night, mini-maxi) in greenhouse. Well-watered conditions were kept until plants reached the four leaf developmental stage. Then a progressive water deficit was applied. Each pot was placed on a scale with automated irrigation to impose the targeted soil water potential. LER was measured when the tip of the $6^{th}$ leaf appeared above the whorl and lasted until the appearance of leaf 8. LER was expressed in thermal time, via equivalent days at 20℃ according to Parent et al. (2010). $\Psi_{leaf}$ was measured with a pressure chamber between 12:00-14:00 in the greenhouse with non-expanding leaves.

**Inference on radial patterns of cell membrane permeability**

In order to test hypotheses on the radial pattern of plasma membrane permeability, we simulated how measured cell-scale permeability ($L_{pc}$) translates into root hydraulic conductivity ($L_{pr}$) for each pattern, and compared the distributions of simulated and measured $L_{pr}$.

Assuming that the axial resistance to water flow is negligible, the simulation framework MECHA (Couvreur et al., 2018) estimates $L_{pr}$ from root transverse anatomy and subcellular scale hydraulic properties. In order to plug the measured $L_{pc}$ into the model, we partitioned it into its two main components: the plasma membrane hydraulic conductivity ($k_{AQP}$, including the contribution of aquaporins) and the conductance of plasmodesmata per unit membrane surface ($k_{PD}$). The latter parameter was assumed to equal $2.4\times10^{-7}$ $m.s^{-1}.MPa^{-1}$ following

(Couvreur et al., 2018), based on plasmodesmata frequency data from Ma and Peterson (2001) and the low range of plasmodesmata conductance estimated by Bret-Harte and Silk (1994). This value was subtracted from the measured $L_{pc}$ to obtain $k_{AQP}$. As the value of the cell wall hydraulic conductivity parameter ($k_w$) is highly uncertain, a range of "low" ($k_{w1}$ = $6.9\times10^{-11}$ $m^2.s^{-1}.MPa^{-1}$), "medium" ($k_{w2}$ = $6.9\times10^{-10}$ $m^2.s^{-1}.MPa^{-1}$), and "high" ($k_{w3}$ = $1.4\times10^{-8}$ $m^2.s^{-1}.MPa^{-1}$) values were tested. Finally, the hydrophobic wall segments of Casparian strips in the endodermis and exodermis were attributed to null hydraulic conductivity. As experimental observations confirmed that root anatomy only varied slightly between the tested lines, the same geometrical layout was used for all of them, except for the mutant PIP2;5 OE-13 whose cell sizes were multiplied by 1.17, as observed experimentally. The anatomy was representative of a maize primary root (0.9 mm diameter), five centimeters proximal to the tip. For details, see Couvreur et al. (2018). In the future, it will be possible to generate anatomies more representative of each mutant with the tool GRANAR (Heymans et al., 2019).

In hypothesis A we assumed that plasma membrane permeability ($k_{AQP}$) is radially uniform and equal to that measured in cortical cells, in WT, PIP2;5 OE and *pip2;5* KO lines, respectively (Fig. 4A). In hypothesis B we assumed that while $k_{AQP}$ uniformly saturates in the PIP2;5 OE lines, it also saturates in the endodermis and exodermis of the WT (Fig. 4E). Besides, in this hypothesis we also assumed that since PIP2;5 is not the only aquaporin highly expressed in the endodermis and exodermis, these cell layers may retain $k_{AQP}$ values as high as half of the saturated values in the *pip2;5* KO line (Fig. 4E).

$L_{pr}$ values were estimated with MECHA for each combination of measured $L_{pc}$ (10 to 14 repetitions) by hypothesized radial pattern (2) by WT or PIP2;5 deregulated lines (6) by cell wall hydraulic conductivity value (3). Relative $L_{pr}$ were calculated by dividing the $L_{pr}$ in WT and associated deregulated line by the average $L_{pr}$ of the WT line. A lognormal transformation was applied to the relative $L_{pr}$ in order to correct for the skewness of their distributions in the following statistical analyses. Contrasts between measured and simulated relative $L_{pr}$ in WT and associated deregulated lines were then investigated with ANOVA2 functions in the software SAS (SAS Institute, Inc., Cary, North Carolina). The contrast between measured $L_{pr}$ in WT and PIP2;5 deregulated lines was considered significantly different from the contrast between simulated $L_{pr}$ in WT and deregulated lines starting at a *p*-value of 0.05.

## Statistical analysis

Student's t test was applied to determine the significance of differences of average values between the PIP2;5 OE/KO lines and their respective WT plants. In Fig. 4 and 5B, one-way ANOVA with Tukey post test was used to compare leaf water potential between WT-B104 and PIP2;5 OE-4 plants under control and water deficit conditions.

## Accession numbers

All accession numbers of the genes are listed in Supplemental Table S2.

## Acknowledgements

We thank Lucie Bugeia for her help in performing the LER measurement in the *Phenodyn*

platform.

**Supplemental Data**

**Supplemental Figure S1.** Levels of PIP transcripts in WT, PIP2;5 OE-4, PIP2;5 OE-13 and *pip2;5* KO lines in roots and leaves.

**Supplemental Figure S2.** RT-PCR amplification of *PIP2;5*.

**Supplemental Figure S3.** Comparison of PIP1;2 and PIP2;1/2;2 protein levels in WT-B104 and PIP2;5 OE lines or WT-W22 and *pip2;5* KO line

**Supplemental Figure S4.** Localization and expression of PIP2;5 in W22 line.

**Supplemental Figure S5.** Mean leaf elongation rate (LER) in the night and day.

**Supplemental Figure S6.** Comparison of $L_{pr}$ between WT-B104 and PIP2;5 OE-4 line under control and PEG treatments.

**Supplemental Table S1.** Primers used for the RT-qPCR experiments.

**Supplemental Table S2. Accession numbers of the genes.**

**Table 1.** Cell pressure probe measurements of maize root cortex cells in WT, PIP2;5 OE lines, and *pip2;5* KO. Root cortical cells from the 3$^{rd}$ to 6$^{th}$ cell layer were punctured in the morning. The values are means ± SE (n = 10~15 cells from three to five plants). Significant difference ($p < 0.05$) among the treatments is indicated by different letters. $T_{1/2}$, the half time of water exchange through the cell membrane. ε, the cell elastic modulus.

| | Turgor pressure (MPa) | $T_{1/2}$ (s) | Cell volume ($10^{-14}$ m$^3$) | Cell surface area ($10^{-8}$ m$^2$) | $\varepsilon_{measured}$ (MPa) | $\varepsilon_{corrected}$ (MPa) |
|---|---|---|---|---|---|---|
| WT-B104 | 0.37±0.01a | 1.70±0.14a | 8.38±1.63a | 1.40±0.17a | 1.24±0.20a | 1.80±0.30a |
| PIP2;5 OE-4 | 0.35±0.01a | 0.89±0.07b | 6.16±1.07a | 1.17±0.12a | 0.89±0.06a | 1.74±0.09a |
| WT-B104 | 0.40±0.01a | 1.75±0.15a | 6.46±0.81b | 1.11±0.09b | 0.98±0.12a | 1.43±0.16b |
| PIP2;5 OE-13 | 0.42±0.01a | 0.97±0.08b | 9.47±0.94a | 1.41±0.10a | 1.49±0.23a | 2.74±0.35a |
| WT-W22 | 0.37±0.01a | 0.90±0.08b | 9.60±0.88a | 1.35±0.09a | 1.38±0.18a | 2.74±0.38a |
| *pip2;5* KO | 0.34±0.02a | 2.56±0.11a | 8.29±0.46a | 1.21±0.05a | 1.61±0.12a | 2.14±0.19a |

## Figure legends

**Figure 1.** PIP2;5 protein levels in the maize lines deregulated in its expression. **A.** Schematic representation of the T-DNA used to overexpress PIP2;5 in the B104 maize line. *p*35S, 35S promoter; YFP, yellow fluorescent proteins; *tnos*, terminator of the nopaline gene; *bar*, the gene conferring resistance to bialaphos. **B.** Genomic structure of the *PIP2;5* gene with the position of the Mu transposon insertion in the *pip2;5* KO line (W22 background). The data source of gene position and insertion site is from "Maize B73 RefGen_v3" in MaizeGDB (https://maizegdb.org/). The *PIP2;5* exons are in red. **C** and **D.** PIP2;5 protein level in root (**C**) and leaf (**D**) in wild type (WT, indicated by WT-B104 and WT-W22), two PIP2;5 overexpressing lines (PIP2;5 OE-4 and OE-13), and *pip2;5* knockout line (*pip2;5* KO). The plants were cultured under hydroponic conditions and the microsomal fractions were extracted from primary roots and leaves of one-week old seedlings. Proteins (20 µg (C) or 30 µg (D)) were subjected to Western blotting using antibodies raised against PIP2;5 or PMA ($H^+$-ATPases). The PMA signal was used to control the gel loading and normalize the PIP2;5 signals (right panels). In the quantification panels, data are expressed as the mean ± SE coming from two independent experiments and each experiment containing two to three plants for each maize line. Significant differences among the treatments are indicated by * ($p<0.05$), ** ($p<0.01$), and *** ($p<0.001$).

**Figure 2.** Membrane water permeability of root cortex cells and leaf mesophyll cells. Hydraulic conductivity of root cortical cells ($L_{pc}$, A-C) and the osmotic water permeability coefficient of leaf mesophyll cell protoplasts ($P_{os}$, D-F) in WT, PIP2;5 OE-4, PIP2;5 OE-13, and *pip2;5* KO line. One- and three-week old plants grown under hydroponic conditions were used for the measurements of $L_{pc}$ and $P_{os}$, respectively. Individual data dots are shown and data are also expressed as the mean ± SE of 10 to 15 cells from three to five plants for the $L_{pc}$ and more than 30 protoplasts coming from two plants for the $P_{os}$. Significant differences among the treatments are indicated by * ($p<0.05$), ** ($p<0.01$), and *** ($p<0.001$). ns indicates not significantly different ($p>0.05$).

**Figure 3.** Root hydraulic conductivity and leaf hydraulic conductance. Root hydraulic conductivity ($L_{pr}$, A-C) and the leaf hydraulic conductance ($K_{leaf}$, D-F) in WT, PIP2;5 OE-4, PIP2;5 OE-13, and *pip2;5* KO line. $L_{pr}$ was measured with two-week old maize seedlings and $K_{leaf}$ of newly expanded leaves was measured with three-week old plants. Individual data dot are shown and data are also expressed as the mean ± SE of roots and leaves from 4 to 6 plants. Significant differences among the treatments are indicated by * ($p<0.05$) and ** ($p<0.01$). ns indicates not significantly different ($p>0.05$).

**Figure 4.** Contrast analysis between experimental and simulated $L_{pr}$ using the MECHA model. Contrast analysis between measured (Exp) and simulated ($k_{w1}$, $k_{w2}$, and $k_{w3}$) $L_{pr}$ in WT (blue) and *PIP2;5* deregulated lines (red: *pip2;5* KO; green: PIP2;5 OE) for hypothesized radial patterns of plasma membrane permeability ($k_{AQP}$). * and ** for significantly different contrasts between measurements and simulations ($p < 0.05$ and 0.001; e.g. contrast between WT and OE larger in simulations than experiments in panel B). Circles/bars: $25^{th}$, $50^{th}$, $75^{th}$

percentiles; Whiskers: most extreme non-outlier data point.

**Figure 5.** Daily time courses of environmental conditions, leaf water potential, and leaf elongation rate under well-watered and moderate water deficit treatments. In this experiment, wild type (WT-B104) and PIP2;5 overexpression line (PIP2;5 OE-4) were compared. In A, blue and red traces indicate vapor pressure deficit (VPD) and photosynthetic photon flux density (PPFD), respectively. In B, white and grey filled bars show leaf water potential of WT-B104 and PIP2;5 OE-4, respectively, under control and water deficit conditions. In C and D, blue and red traces show the leaf elongation rate (LER) of WT-B104 and PIP2;5 OE-4, respectively. Gray traces show the daily soil water potential ($\Psi_{soil}$). Gray backgrounds show the sunset period. In dashed line square, the slope rate is analyzed, and the result is inserted. LER is expressed per unit thermal time ($mm.h^{-1}_{20^oC}$). Error bars indicate standard error (n= 3~9 plants). In B, one-way ANOVA with Tukey post test is used to compare the significant differences between WT-B104 and PIP2;5 OE-4 plants under control and water deficit conditions. Significant differences are indicated by different letters ($p<0.05$). In the insert of D, Student`s t-test is used to compare the significant difference between WT-B104 and PIP2;5 OE-4 plants. * indicates the significant difference at level of $p<0.05$.

## Literature Cited


**Avramova V, Sprangers K, Beemster GT** (2015) The maize leaf: another perspective on growth regulation. Trends in Plant Science **20:** 787-797

**Besserer A, Burnotte E, Bienert GP, Chevalier AS, Errachid A, Grefen C, Blatt MR, Chaumont F** (2012) Selective regulation of maize plasma membrane aquaporin trafficking and activity by the SNARE SYP121. The Plant Cell **24:** 3463-3481

**Bouchabké O, Tardieu F, Simonneau T** (2006) Leaf growth and turgor in growing cells of maize (Zea mays L.) respond to evaporative demand under moderate irrigation but not in water-saturated soil. Plant, Cell & Environment **29:** 1138-1148

**Bradford MM** (1976) A rapid and sensitive method for the quantitation of microgram quantities of protein utilizing the principle of protein-dye binding. Analytical biochemistry **72:** 248-254

**Bret-Harte MS, Silk WK** (1994) Nonvascular, symplasmic diffusion of sucrose cannot satisfy the carbon demands of growth in the primary root tip of Zea mays L. Plant Physiology **105:** 19-33

**Buckley TN** (2015) The contributions of apoplastic, symplastic and gas phase pathways for water transport outside the bundle sheath in leaves. Plant, Cell & Environment **38:** 7-22

**Caldeira CF, Bosio M, Parent B, Jeanguenin L, Chaumont F, Tardieu F** (2014) A hydraulic model is compatible with rapid changes in leaf elongation under fluctuating evaporative demand and soil water status. Plant Physiology **164:** 1718-1730

**Caldeira CF, Jeanguenin L, Chaumont F, Tardieu F** (2014) Circadian rhythms of hydraulic conductance and growth are enhanced by drought and improve plant performance.

Nature communications **5:** 5365-5365
**Chaumont F, Tyerman SD** (2014) Aquaporins: highly regulated channels controlling plant water relations. Plant Physiology **164:** 1600-1618
**Coussens G, Aesaert S, Verelst W, Demeulenaere M, De Buck S, Njuguna E, Inzé D, Van Lijsebettens M** (2012) Brachypodium distachyon promoters as efficient building blocks for transgenic research in maize. Journal of experimental botany **63:** 4263-4273
**Couvreur V, Faget M, Lobet G, Javaux M, Chaumont F, Draye X** (2018) Going with the flow: multiscale insights into the composite nature of water transport in roots. Plant physiology **178:** 1689-1703
**Curtis MD, Grossniklaus U** (2003) A gateway cloning vector set for high-throughput functional analysis of genes in planta. Plant Physiology **133:** 462-469
**Ding L, Gao C, Li Y, Li Y, Zhu Y, Xu G, Shen Q, Kaldenhoff R, Kai L, Guo S** (2015) The enhanced drought tolerance of rice plants under ammonium is related to aquaporin (AQP). Plant Science **234:** 14-21
**Ferrio JP, Pou A, FLOREZ-SARASA I, Gessler A, Kodama N, Flexas J, RIBAS-CARBÓ M** (2012) The Péclet effect on leaf water enrichment correlates with leaf hydraulic conductance and mesophyll conductance for CO2. Plant, Cell & Environment **35:** 611-625
**Fetter K, Van Wilder V, Moshelion M, Chaumont F** (2004) Interactions between plasma membrane aquaporins modulate their water channel activity. The Plant Cell **16:** 215-228
**Foster KJ, Miklavcic SJ** (2017) A comprehensive biophysical model of ion and water transport in plant roots. I. Clarifying the roles of endodermal barriers in the salt stress response. Frontiers in plant science **8:** 1326
**Grondin A, Rodrigues O, Verdoucq L, Merlot S, Leonhardt N, Maurel C** (2015) Aquaporins contribute to ABA-triggered stomatal closure through OST1-mediated phosphorylation. The Plant Cell **27:** 1945-1954
**Hachez C, Heinen RB, Draye X, Chaumont F** (2008) The expression pattern of plasma membrane aquaporins in maize leaf highlights their role in hydraulic regulation. Plant molecular biology **68:** 337
**Hachez C, Moshelion M, Zelazny E, Cavez D, Chaumont F** (2006) Localization and quantification of plasma membrane aquaporin expression in maize primary root: a clue to understanding their role as cellular plumbers. Plant molecular biology **62:** 305-323
**Hachez C, Veselov D, Ye Q, Reinhardt H, Knipfer T, Fricke W, Chaumont F** (2012) Short-term control of maize cell and root water permeability through plasma membrane aquaporin isoforms. Plant, cell & environment **35:** 185-198
**Hachez C, Zelazny E, Chaumont F** (2006) Modulating the expression of aquaporin genes in planta: a key to understand their physiological functions? Biochimica et Biophysica Acta (BBA)-Biomembranes **1758:** 1142-1156
**Hebelstrup KH, Christiansen MW, Carciofi M, Tauris B, Brinch-Pedersen H, Holm PB** (2010) UCE: A uracil excision (USER™)-based toolbox for transformation of cereals. Plant Methods **6:** 15
**Heinen RB, Bienert GP, Cohen D, Chevalier AS, Uehlein N, Hachez C, Kaldenhoff R, Le Thiec D, Chaumont F** (2014) Expression and characterization of plasma membrane

aquaporins in stomatal complexes of Zea mays. Plant molecular biology **86:** 335-350

**Heinen RB, Ye Q, Chaumont F** (2009) Role of aquaporins in leaf physiology. Journal of experimental botany **60:** 2971-2985

**Heymans A, Couvreur V, LaRue T, Paez-Garcia A, Lobet G** (2019) GRANAR, a new computational tool to better understand the functional importance of root anatomy. bioRxiv**:** 645036

**Hood EE, Helmer G, Fraley R, Chilton MD** (1986) The hypervirulence of Agrobacterium tumefaciens A281 is encoded in a region of pTiBo542 outside of T-DNA. Journal of Bacteriology **168:** 1291-1301

**Hunter CT, Suzuki M, Saunders J, Wu S, Tasi A, McCarty DR, Koch KE** (2014) Phenotype to genotype using forward-genetic Mu-seq for identification and functional classification of maize mutants. Frontiers in plant science **4:** 545

**Javot H, Lauvergeat V, Santoni V, Martin-Laurent F, Güçlü J, Vinh J, Heyes J, Franck KI, Schäffner AR, Bouchez D** (2003) Role of a single aquaporin isoform in root water uptake. The plant cell **15:** 509-522

**Karimi M, Inzé D, Van Lijsebettens M, Hilson P** (2013) Gateway vectors for transformation of cereals. Trends in plant science **18:** 1-4

**Kubo M, Udagawa M, Nishikubo N, Horiguchi G, Yamaguchi M, Ito J, Mimura T, Fukuda H, Demura T** (2005) Transcription switches for protoxylem and metaxylem vessel formation. Genes & development **19:** 1855-1860

**Lee SH, Chung GC, Jang JY, Ahn SJ, Zwiazek JJ** (2012) Overexpression of PIP2; 5 aquaporin alleviates effects of low root temperature on cell hydraulic conductivity and growth in Arabidopsis. Plant physiology **159:** 479-488

**Ma F, Peterson CA** (2001) Frequencies of plasmodesmata in Allium cepa L. roots: implications for solute transport pathways. Journal of Experimental Botany **52:** 1051-1061

**Maurel C, Boursiac Y, Luu D-T, Santoni V, Shahzad Z, Verdoucq L** (2015) Aquaporins in plants. Physiological reviews **95:** 1321-1358

**Maurel C, Verdoucq L, Rodrigues O** (2016) Aquaporins and plant transpiration. Plant, cell & environment **39:** 2580-2587

**McCarty DR, Mark Settles A, Suzuki M, Tan BC, Latshaw S, Porch T, Robin K, Baier J, Avigne W, Lai J** (2005) Steady-state transposon mutagenesis in inbred maize. The Plant Journal **44:** 52-61

**McCarty DR, Suzuki M, Hunter C, Collins J, Avigne WT, Koch KE** (2013) Genetic and molecular analyses of UniformMu transposon insertion lines. *In* Plant Transposable Elements. Springer, pp 157-166

**Morsomme P, de Kerchove d'Exaerde A, De Meester S, Thines D, Goffeau A, Boutry M** (1996) Single point mutations in various domains of a plant plasma membrane H (+)-ATPase expressed in Saccharomyces cerevisiae increase H (+)-pumping and permit yeast growth at low pH. The EMBO Journal **15:** 5513-5526

**Moshelion M, Moran N, Chaumont F** (2004) Dynamic changes in the osmotic water permeability of protoplast plasma membrane. Plant Physiology **135:** 2301-2317

**Nelissen H, Rymen B, Jikumaru Y, Demuynck K, Van Lijsebettens M, Kamiya Y, Inzé D, Beemster GT** (2012) A local maximum in gibberellin levels regulates maize leaf

855 growth by spatial control of cell division. Current Biology **22:** 1183-1187
856 **Nelissen H, Sun XH, Rymen B, Jikumaru Y, Kojima M, Takebayashi Y, Abbeloos R,**
857 **Demuynck K, Storme V, Vuylsteke M** (2018) The reduction in maize leaf growth
858 under mild drought affects the transition between cell division and cell expansion and
859 cannot be restored by elevated gibberellic acid levels. Plant Biotechnology Journal **16:**
860 615-627
861 **Nour-Eldin HH, Hansen BG, Nørholm MH, Jensen JK, Halkier BA** (2006) Advancing
862 uracil-excision based cloning towards an ideal technique for cloning PCR fragments.
863 Nucleic Acids Research **34:** e122-e122
864 **Parent B, Hachez C, Redondo E, Simonneau T, Chaumont F, Tardieu F** (2009) Drought
865 and abscisic acid effects on aquaporin content translate into changes in hydraulic
866 conductivity and leaf growth rate: a trans-scale approach. Plant Physiology **149:**
867 2000-2012
868 **Parent B, Turc O, Gibon Y, Stitt M, Tardieu F** (2010) Modelling temperature-compensated
869 physiological rates, based on the co-ordination of responses to temperature of
870 developmental processes. Journal of Experimental Botany **61:** 2057-2069
871 **Péret B, Li G, Zhao J, Band LR, Voß U, Postaire O, Luu D-T, Da Ines O, Casimiro I,**
872 **Lucas M** (2012) Auxin regulates aquaporin function to facilitate lateral root
873 emergence. Nature cell biology **14:** 991
874 **Postaire O, Tournaire-Roux C, Grondin A, Boursiac Y, Morillon R, Schaffner AR,**
875 **Maurel C** (2010) A PIP1 Aquaporin Contributes to Hydrostatic Pressure-Induced
876 Water Transport in Both the Root and Rosette of Arabidopsis. Plant Physiology **152:**
877 1418-1430
878 **Prado K, Maurel C** (2013) Regulation of leaf hydraulics: from molecular to whole plant
879 levels. Frontiers in plant science **4**
880 **Rodrigues O, Reshetnyak G, Grondin A, Saijo Y, Leonhardt N, Maurel C, Verdoucq L**
881 (2017) Aquaporins facilitate hydrogen peroxide entry into guard cells to mediate
882 ABA-and pathogen-triggered stomatal closure. Proceedings of the National Academy
883 of Sciences **114:** 9200-9205
884 **Sack L, Holbrook NM** (2006) Leaf hydraulics. Annu. Rev. Plant Biol. **57:** 361-381
885 **Sade N, Gebretsadik M, Seligmann R, Schwartz A, Wallach R, Moshelion M** (2010) The
886 role of tobacco Aquaporin1 in improving water use efficiency, hydraulic conductivity,
887 and yield production under salt stress. Plant Physiology **152:** 245-254
888 **Sade N, Shatil-Cohen A, Attia Z, Maurel C, Boursiac Y, Kelly G, Granot D, Yaaran A,**
889 **Lerner S, Moshelion M** (2014) The role of plasma membrane aquaporins in
890 regulating the bundle sheath-mesophyll continuum and leaf hydraulics. Plant
891 Physiology **166:** 1609-1620
892 **Sadok W, Naudin P, Boussuge B, Muller B, Welcker C, Tardieu F** (2007) Leaf growth rate
893 per unit thermal time follows QTL-dependent daily patterns in hundreds of maize lines
894 under naturally fluctuating conditions. Plant, Cell & Environment **30:** 135-146
895 **Shatil-Cohen A, Sibony H, Draye X, Chaumont F, Moran N, Moshelion M** (2014)
896 Measuring the osmotic water permeability coefficient (Pf) of spherical cells: isolated
897 plant protoplasts as an example. Journal of visualized experiments: JoVE
898 **Shatil-Cohen A, Attia Z, Moshelion M** (2011) Bundle-sheath cell regulation of xylem-

mesophyll water transport via aquaporins under drought stress: a target of xylem-borne ABA? The Plant Journal **67:** 72-80

**Siefritz F, Tyree MT, Lovisolo C, Schubert A, Kaldenhoff R** (2002) PIP1 plasma membrane aquaporins in tobacco from cellular effects to function in plants. The Plant Cell **14:** 869-876

**Steudle E** (2000) Water uptake by plant roots: an integration of views. Plant and Soil **226:** 45-56

**Steudle E, Peterson CA** (1998) How does water get through roots? Journal of Experimental Botany **49:** 775-788

**Tyree MT, Nardini A, Salleo S, Sack L, El Omari B** (2004) The dependence of leaf hydraulic conductance on irradiance during HPFM measurements: any role for stomatal response? Journal of Experimental Botany **56:** 737-744

**Volkov V, Fricke W, Hachez C, Moshelion M, Draye X, Chaumont F** (2006) Osmotic water permeability differs between growing and non-growing barley leaf tissues. Comparative Biochemistry and Physiology a-Molecular & Integrative Physiology **143:** S48-S48

**Wang C, Hu H, Qin X, Zeise B, Xu D, Rappel W-J, Boron WF, Schroeder JI** (2016) Reconstitution of CO2 regulation of SLAC1 anion channel and function of CO2-permeable PIP2; 1 aquaporin as CARBONIC ANHYDRASE4 interactor. The Plant Cell **28:** 568-582

**Zwieniecki MA, Thompson MV, Holbrook NM** (2002) Understanding the hydraulics of porous pipes: tradeoffs between water uptake and root length utilization. Journal of Plant Growth Regulation **21:** 315-323

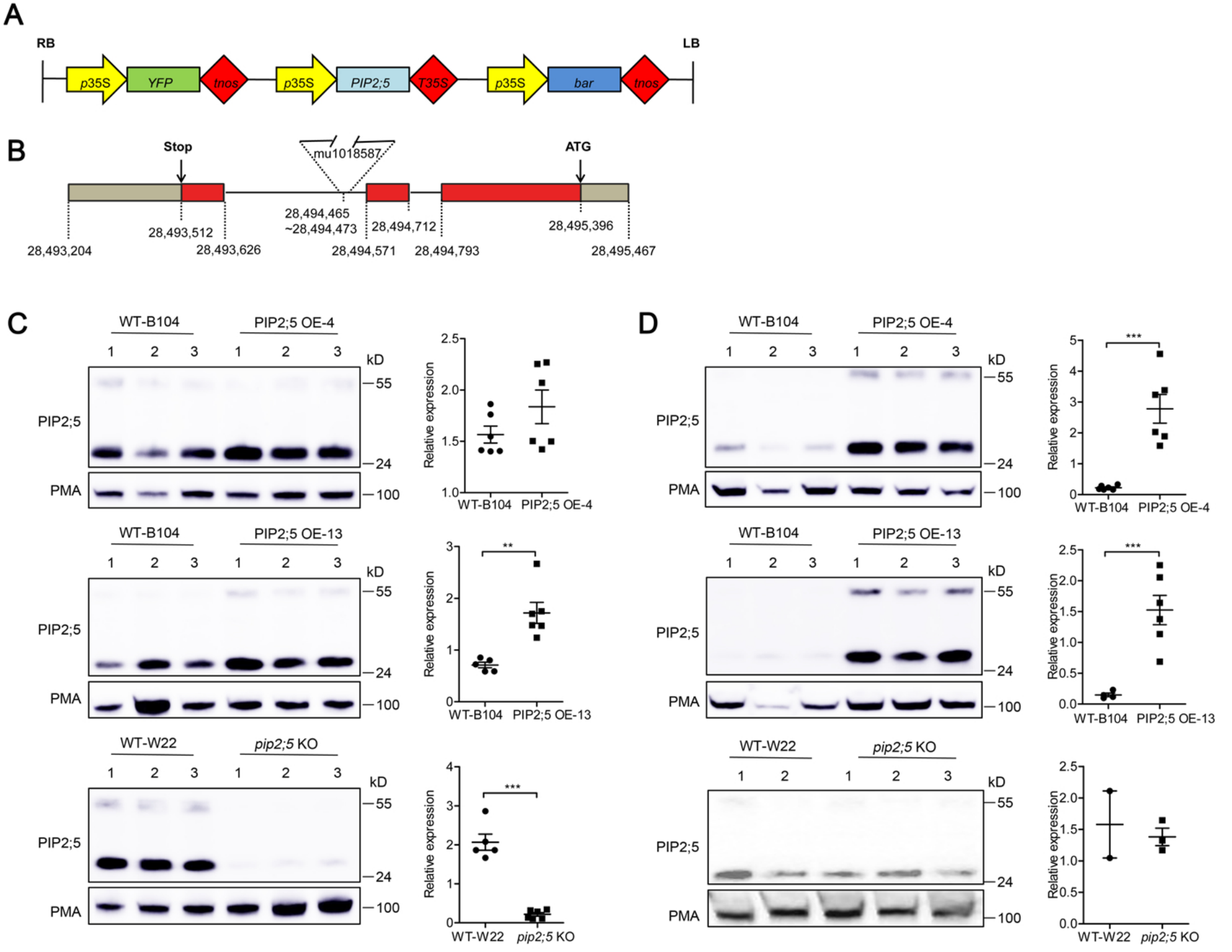


Figure 1. A. Schematic representation of the T-DNA used to overexpress PIP2;5 in the B104 maize line. *p35S*, 35S promoter; YFP, yellow fluorescent proteins; tnos, terminator of thenopaline gene; bar, the gene conferring resistance to bialaphos. B. Genomic structure of the PIP2;5 gene with the position of the Mu transposon insertion in the *pip2;5* KO line (W22 background). The data source of gene position and insertion site is from "Maize B73 RefGen_v3" in MaizeGDB (https://maizegdb.org/). The PIP2;5 exons are in red. C and D. PIP2;5 protein level in root (C) and leaf (D) in wild type (WT, indicated by WT-B104 and WT-W22), two PIP2;5 overexpressing lines (PIP2;5 OE-4 and OE-13) and *pip2;5* knockout line (*pip2;5* KO). The plants were cultured in hydroponic condition and the microsomal fractions were extracted from primary roots and leaves of one week-old seedlings. Proteins (20 µg (C) or 30 µg (D)) were subjected to Western blotting using antibodies raised against PIP2;5 or PMA ($H^+$-ATPases). The PMA signal was used to control the gel loading and normalize the PIP2;5 signals (gray panels). In the quantification panels, data are expressed as the mean ± SE coming from two independent experiments and each experiment containing two to three plants for each genotype. Significant differences among the treatments are indicated by * ($p<0.05$), ** ($p<0.01$) and *** ($p<0.001$).

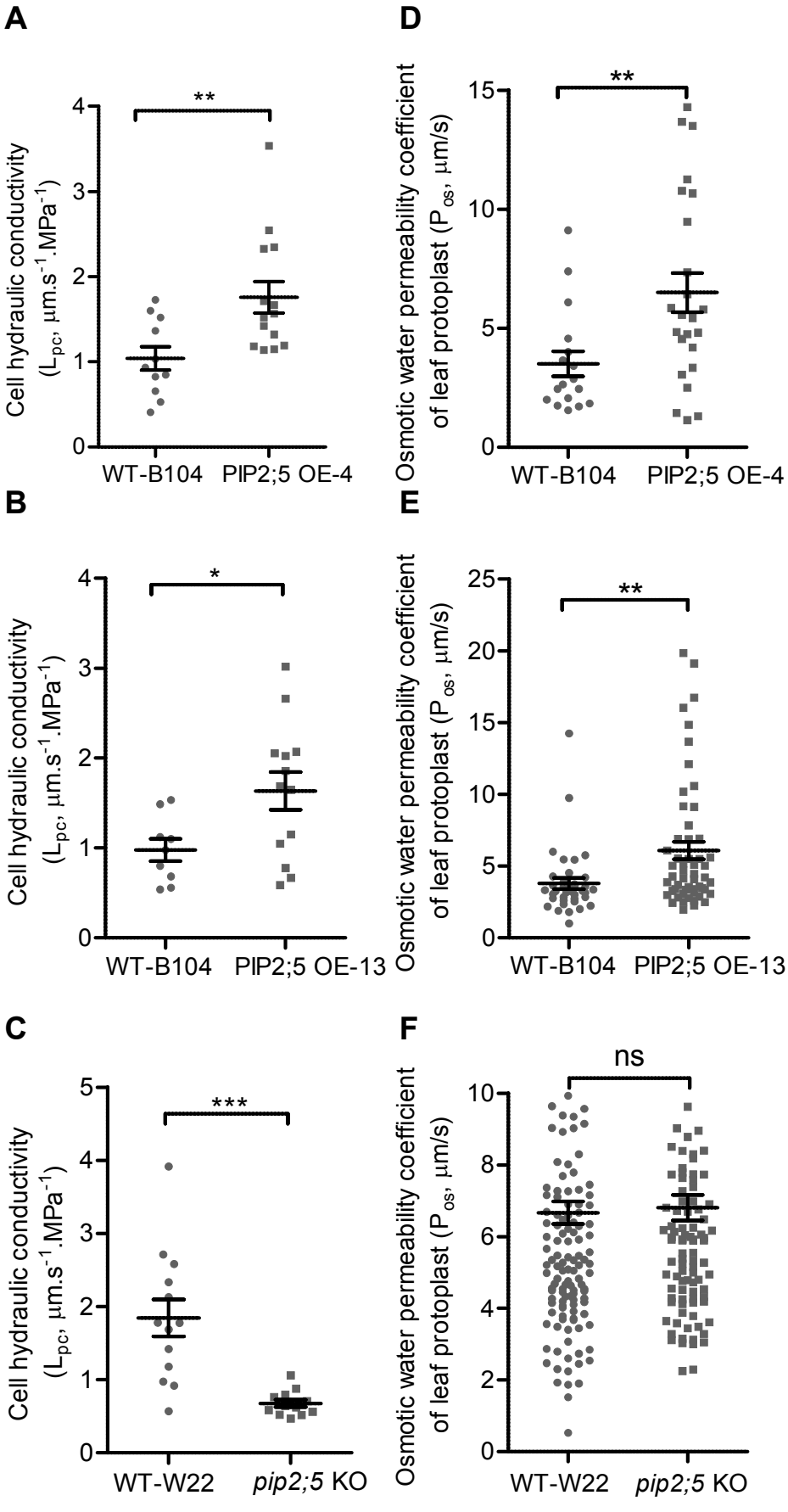


**Figure 2.** Hydraulic conductivity of root cortical cells ($L_{pc}$, A-C) and the osmotic water permeability coefficient of leaf mesophyll cells protoplasts ($P_{os}$, D-F) in WT, PIP2;5 OE-4, PIP2;5 OE-13 and *pip2;5* KO line. One-and-three-week old plants growing in hydroponic condition were used for the measurements of $L_{pc}$ and $P_{os}$, respectively. Individual data dots are shown and data are also expressed as the mean ± SE of 10 to 15 cells from three to five plants for the Lpc and more than 30 protoplasts coming from two plants for the $P_{os}$. Significant differences among the treatments are indicated by * ($p<0.05$), ** ($p<0.01$) and *** ($p<0.001$), respectively. ns indicates not significantly different ($p<0.05$).

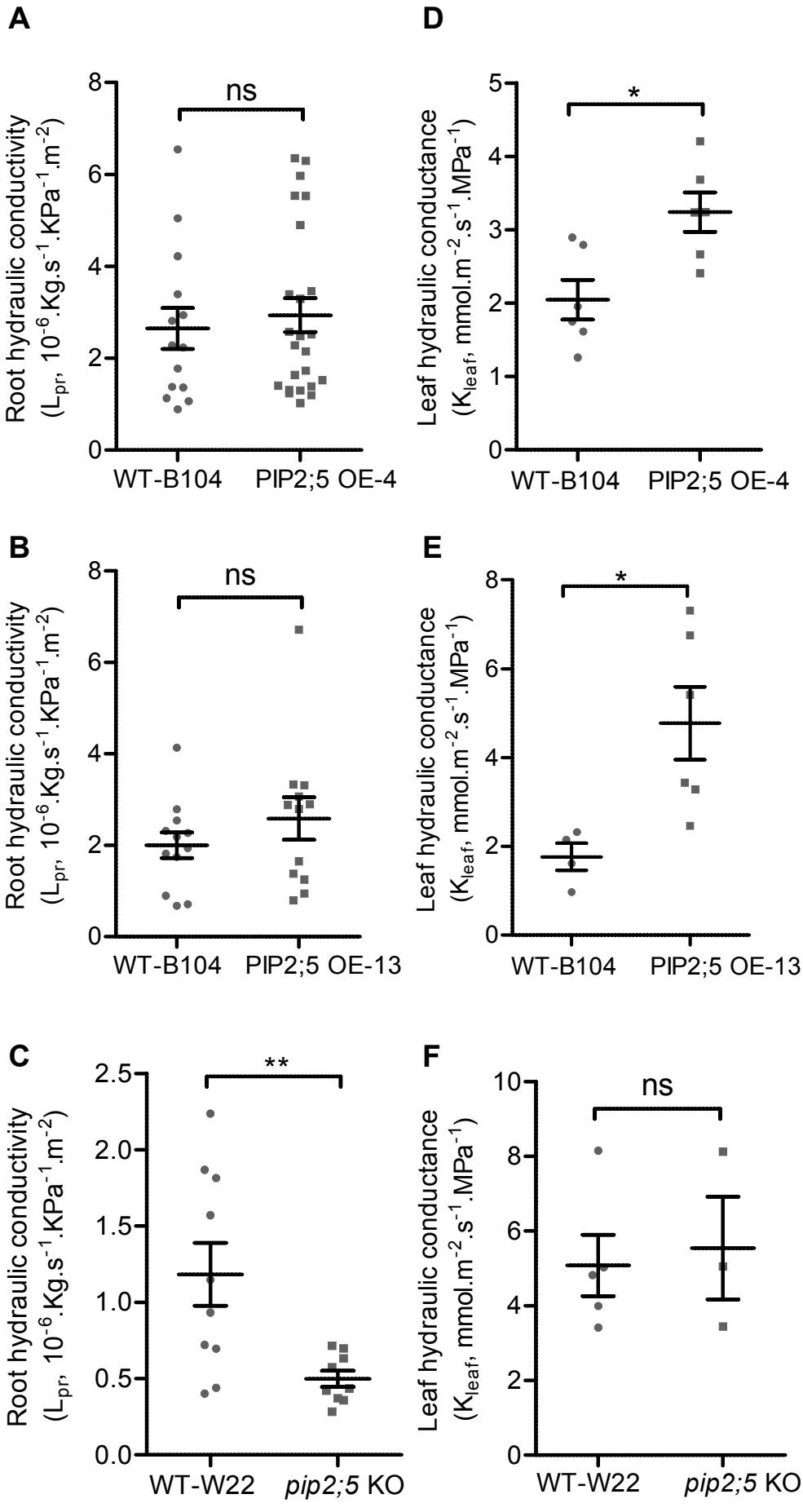


**Figure 3**. Root hydraulic conductivity ($L_{pr}$, A-C) and the leaf hydraulic conductance ($K_{leaf}$, D-F) in WT, PIP2;5 OE-4, PIP2;5 OE-13 and *pip2;5* KO line. $L_{pr}$ was measured with two-week old maize seedlings and $K_{leaf}$ of newly expanded leaf was measured with three-week old plants. Individual data dots are shown and data are also expressed as the mean ± SE of roots and leaves from 4 to 6 plants. Significant differences between WT and PIP2;5 deregulation plants are indicated by * ($p<0.05$) and ** ($p<0.01$) or ns indicates not significantly different ($p<0.05$).

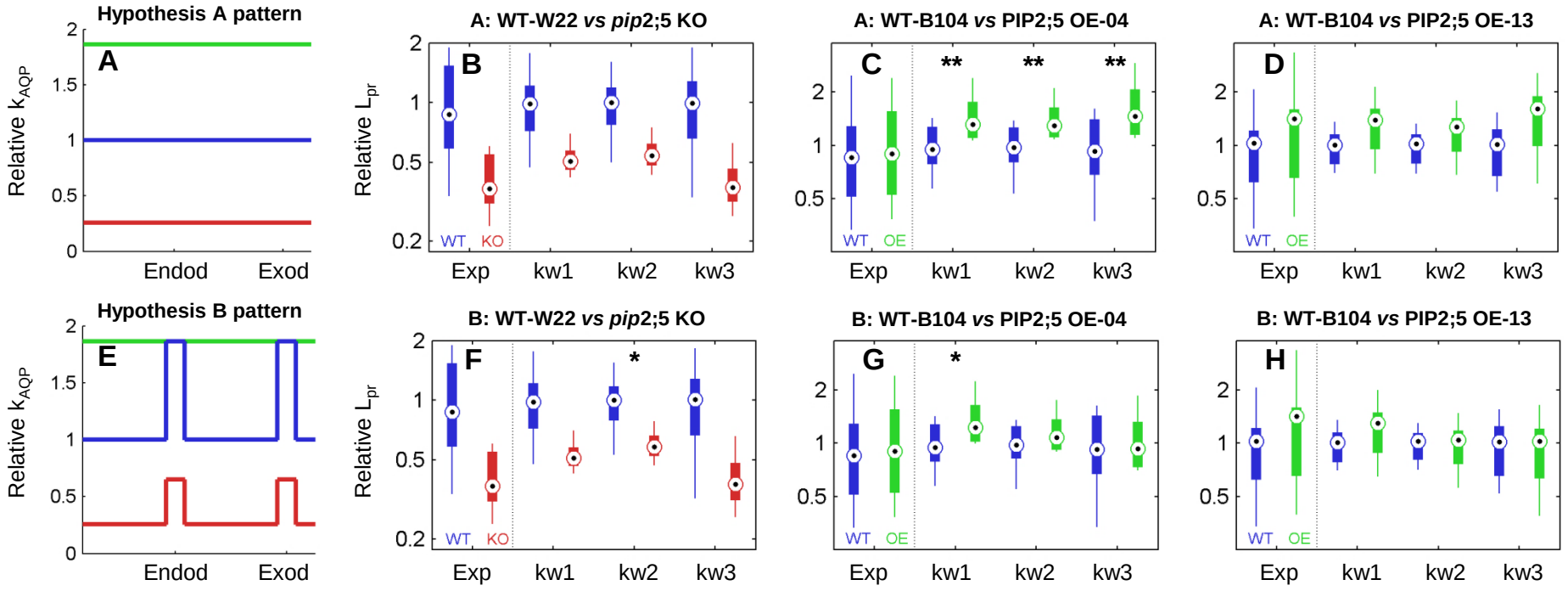


**Figure 4.** Contrast analysis between measured (Exp) and simulated ($k_{w1}$, $k_{w2}$ and $k_{w3}$) $L_{pr}$ in WT (blue) and PIP2;5 deregulated lines (red: *pip2;5* KO; green: PIP2;5 OE) for hypothesized radial patterns of plasmalemma permeability ($k_{AQP}$). * and ** for significantly different contrasts between measurements and simulations ($p < 0.05$ and 0.001; e.g. contrast between WT and OE targets in simulations than experiments in panel B). Circles/bars: 25th, 50th, 75th percentiles; Whiskers: most extreme non-outlier data point.

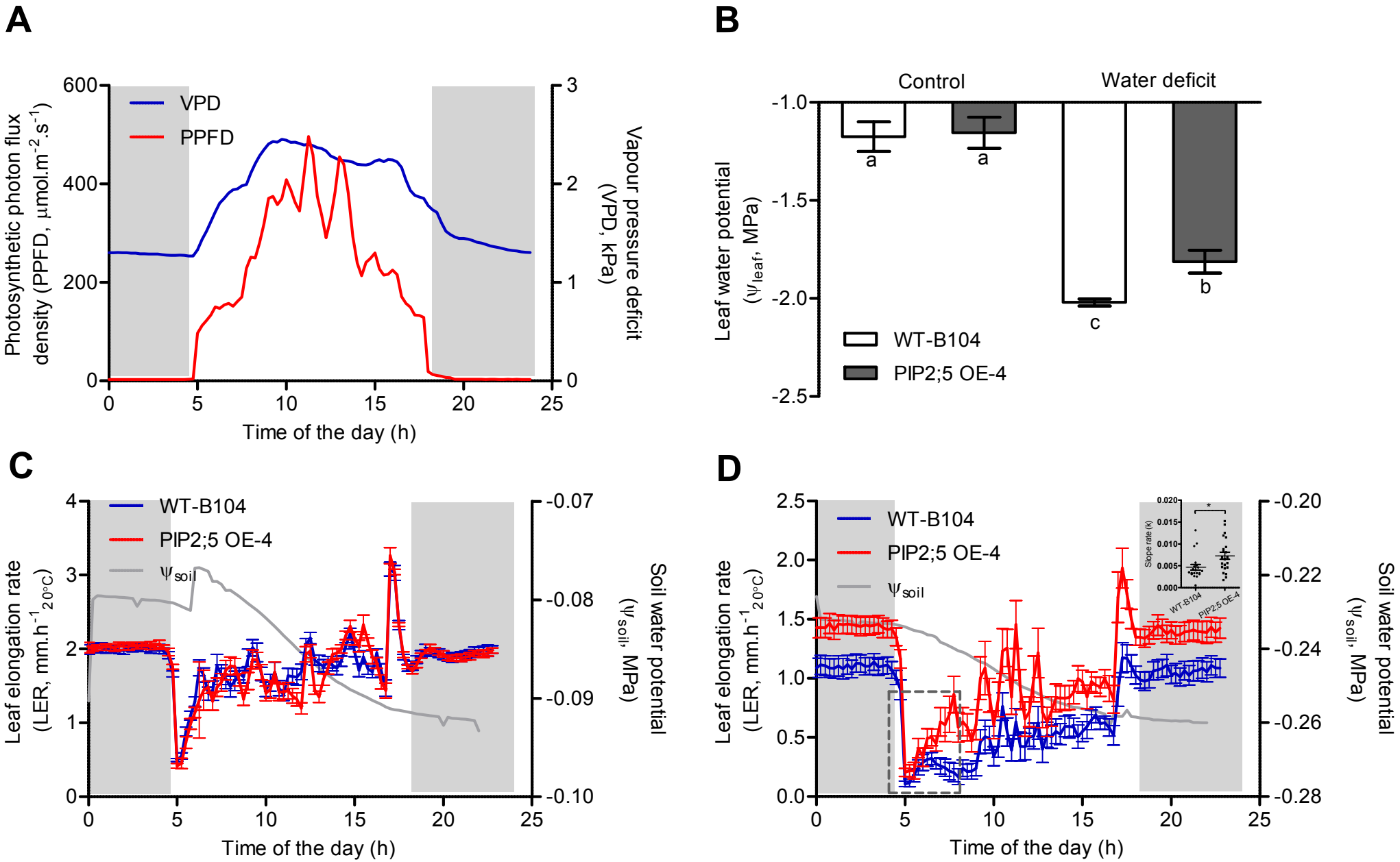


**Figure 5.** Daily time courses of environmental conditions (A), leaf water potential (B) and leaf elongation rate (LER) under well-watered (C) and moderate water deficit (D) treatments. In this experiment, wild type (WT-B104) and PIP2;5 overexpression line (PIP2;5 OE-4) were compared. In A, blue and red trace shows vapor pressure deficit (VPD) and photosynthetic photon flux density (PPFD), respectively. In B, white and grey filled bars show leaf water potential of WT-B104 and PIP2;5 OE-4, respectively, under control and water deficit conditions. In C and D, blue and red traces show the LER of WT-B104 and PIP2;5 OE-4, respectively. Gray traces show the daily soil water potential ($\psi_{soil}$). Gray backgrounds show the sunset period. In dashed line square, the slope rate is analyzed, and the result is inserted. LER is expressed per unit thermal time ($mm.h^{-1}_{20°C}$). Error bars indicate standard error (n= 3~9 plants). In B, one-way ANOVA with Tukey post test is used to compare the significant differences betwen WT-B104 and PIP2;5 OE-4 plants under control and water deficit conditions. Significant difference is indicated by different letters ($p<0.05$). In the inset of D, Student`s t-test is used to compare the significant difference between WT-B104 and PIP2;5 OE-4 plants. * indicates the significant difference at level of $p<0.05$.

## Parsed Citations


**Avramova V, Sprangers K, Beemster GT (2015) The maize leaf: another perspective on growth regulation. Trends in Plant Science 20: 787-797**

Pubmed: Author and Title
Google Scholar: Author Only Title Only Author and Title

**Besserer A, Burnotte E, Bienert GP, Chevalier AS, Errachid A, Grefen C, Blatt MR, Chaumont F (2012) Selective regulation of maize plasma membrane aquaporin trafficking and activity by the SNARE SYP121. The Plant Cell 24: 3463-3481**

Pubmed: Author and Title
Google Scholar: Author Only Title Only Author and Title

**Bouchabké O, Tardieu F, Simonneau T (2006) Leaf growth and turgor in growing cells of maize (Zea mays L.) respond to evaporative demand under moderate irrigation but not in water-saturated soil. Plant, Cell & Environment 29: 1138-1148**

Pubmed: Author and Title
Google Scholar: Author Only Title Only Author and Title

**Bradford MM (1976) A rapid and sensitive method for the quantitation of microgram quantities of protein utilizing the principle of protein-dye binding. Analytical biochemistry 72: 248-254**

Pubmed: Author and Title
Google Scholar: Author Only Title Only Author and Title

**Bret-Harte MS, Silk WK (1994) Nonvascular, symplasmic diffusion of sucrose cannot satisfy the carbon demands of growth in the primary root tip of Zea mays L. Plant Physiology 105: 19-33**

Pubmed: Author and Title
Google Scholar: Author Only Title Only Author and Title

**Buckley TN (2015) The contributions of apoplastic, symplastic and gas phase pathways for water transport outside the bundle sheath in leaves. Plant, Cell & Environment 38: 7-22**

Pubmed: Author and Title
Google Scholar: Author Only Title Only Author and Title

**Caldeira CF, Bosio M, Parent B, Jeanguenin L, Chaumont F, Tardieu F (2014) A hydraulic model is compatible with rapid changes in leaf elongation under fluctuating evaporative demand and soil water status. Plant Physiology 164: 1718-1730**

Pubmed: Author and Title
Google Scholar: Author Only Title Only Author and Title

**Caldeira CF, Jeanguenin L, Chaumont F, Tardieu F (2014) Circadian rhythms of hydraulic conductance and growth are enhanced by drought and improve plant performance. Nature communications 5: 5365-5365**

Pubmed: Author and Title
Google Scholar: Author Only Title Only Author and Title

**Chaumont F, Tyerman SD (2014) Aquaporins: highly regulated channels controlling plant water relations. Plant Physiology 164: 1600-1618**

Pubmed: Author and Title
Google Scholar: Author Only Title Only Author and Title

**Coussens G, Aesaert S, Verelst W, Demeulenaere M, De Buck S, Njuguna E, Inzé D, Van Lijsebettens M (2012) Brachypodium distachyon promoters as efficient building blocks for transgenic research in maize. Journal of experimental botany 63: 4263-4273**

Pubmed: Author and Title
Google Scholar: Author Only Title Only Author and Title

**Couvreur V, Faget M, Lobet G, Javaux M, Chaumont F, Draye X (2018) Going with the flow: multiscale insights into the composite nature of water transport in roots. Plant physiology 178: 1689-1703**

Pubmed: Author and Title
Google Scholar: Author Only Title Only Author and Title

**Curtis MD, Grossniklaus U (2003) A gateway cloning vector set for high-throughput functional analysis of genes in planta. Plant Physiology 133: 462-469**

Pubmed: Author and Title
Google Scholar: Author Only Title Only Author and Title

**Ding L, Gao C, Li Y, Li Y, Zhu Y, Xu G, Shen Q, Kaldenhoff R, Kai L, Guo S (2015) The enhanced drought tolerance of rice plants under ammonium is related to aquaporin (AQP). Plant Science 234: 14-21**

Pubmed: Author and Title
Google Scholar: Author Only Title Only Author and Title

**Ferrio JP, Pou A, FLOREZ-SARASA I, Gessler A, Kodama N, Flexas J, RIBAS-CARBÓ M (2012) The Péclet effect on leaf water enrichment correlates with leaf hydraulic conductance and mesophyll conductance for CO2. Plant, Cell & Environment 35: 611-625**

Pubmed: Author and Title
Google Scholar: Author Only Title Only Author and Title

**Fetter K, Van Wilder V, Moshelion M, Chaumont F (2004) Interactions between plasma membrane aquaporins modulate their water channel activity. The Plant Cell 16: 215-228**

Pubmed: Author and Title
Google Scholar: Author Only Title Only Author and Title

**Foster KJ, Miklavcic SJ (2017) A comprehensive biophysical model of ion and water transport in plant roots. I. Clarifying the roles of endodermal barriers in the salt stress response. Frontiers in plant science 8: 1326**
Pubmed: Author and Title
Google Scholar: Author Only Title Only Author and Title

**Grondin A, Rodrigues O, Verdoucq L, Merlot S, Leonhardt N, Maurel C (2015) Aquaporins contribute to ABA-triggered stomatal closure through OST1-mediated phosphorylation. The Plant Cell 27: 1945-1954**
Pubmed: Author and Title
Google Scholar: Author Only Title Only Author and Title

**Hachez C, Heinen RB, Draye X, Chaumont F (2008) The expression pattern of plasma membrane aquaporins in maize leaf highlights their role in hydraulic regulation. Plant molecular biology 68: 337**
Pubmed: Author and Title
Google Scholar: Author Only Title Only Author and Title

**Hachez C, Moshelion M, Zelazny E, Cavez D, Chaumont F (2006) Localization and quantification of plasma membrane aquaporin expression in maize primary root: a clue to understanding their role as cellular plumbers. Plant molecular biology 62: 305-323**
Pubmed: Author and Title
Google Scholar: Author Only Title Only Author and Title

**Hachez C, Veselov D, Ye Q, Reinhardt H, Knipfer T, Fricke W, Chaumont F (2012) Short-term control of maize cell and root water permeability through plasma membrane aquaporin isoforms. Plant, cell & environment 35: 185-198**
Pubmed: Author and Title
Google Scholar: Author Only Title Only Author and Title

**Hachez C, Zelazny E, Chaumont F (2006) Modulating the expression of aquaporin genes in planta: a key to understand their physiological functions? Biochimica et Biophysica Acta (BBA)-Biomembranes 1758: 1142-1156**
Pubmed: Author and Title
Google Scholar: Author Only Title Only Author and Title

**Hebelstrup KH, Christiansen MW, Carciofi M, Tauris B, Brinch-Pedersen H, Holm PB (2010) UCE: A uracil excision (USER™)-based toolbox for transformation of cereals. Plant Methods 6: 15**
Pubmed: Author and Title
Google Scholar: Author Only Title Only Author and Title

**Heinen RB, Bienert GP, Cohen D, Chevalier AS, Uehlein N, Hachez C, Kaldenhoff R, Le Thiec D, Chaumont F (2014) Expression and characterization of plasma membrane aquaporins in stomatal complexes of Zea mays. Plant molecular biology 86: 335-350**
Pubmed: Author and Title
Google Scholar: Author Only Title Only Author and Title

**Heinen RB, Ye Q, Chaumont F (2009) Role of aquaporins in leaf physiology. Journal of experimental botany 60: 2971-2985**
Pubmed: Author and Title
Google Scholar: Author Only Title Only Author and Title

**Heymans A, Couvreur V, LaRue T, Paez-Garcia A, Lobet G (2019) GRANAR, a new computational tool to better understand the functional importance of root anatomy. bioRxiv: 645036**
Pubmed: Author and Title
Google Scholar: Author Only Title Only Author and Title

**Hood EE, Helmer G, Fraley R, Chilton MD (1986) The hypervirulence of Agrobacterium tumefaciens A281 is encoded in a region of pTiBo542 outside of T-DNA. Journal of Bacteriology 168: 1291-1301**
Pubmed: Author and Title
Google Scholar: Author Only Title Only Author and Title

**Hunter CT, Suzuki M, Saunders J, Wu S, Tasi A, McCarty DR, Koch KE (2014) Phenotype to genotype using forward-genetic Mu-seq for identification and functional classification of maize mutants. Frontiers in plant science 4: 545**
Pubmed: Author and Title
Google Scholar: Author Only Title Only Author and Title

**Javot H, Lauvergeat V, Santoni V, Martin-Laurent F, Güçlü J, Vinh J, Heyes J, Franck KI, Schäffner AR, Bouchez D (2003) Role of a single aquaporin isoform in root water uptake. The plant cell 15: 509-522**
Pubmed: Author and Title
Google Scholar: Author Only Title Only Author and Title

**Karimi M, Inzé D, Van Lijsebettens M, Hilson P (2013) Gateway vectors for transformation of cereals. Trends in plant science 18: 1-4**
Pubmed: Author and Title
Google Scholar: Author Only Title Only Author and Title

**Kubo M, Udagawa M, Nishikubo N, Horiguchi G, Yamaguchi M, Ito J, Mimura T, Fukuda H, Demura T (2005) Transcription switches for protoxylem and metaxylem vessel formation. Genes & development 19: 1855-1860**
Pubmed: Author and Title
Google Scholar: Author Only Title Only Author and Title

**Lee SH, Chung GC, Jang JY, Ahn SJ, Zwiazek JJ (2012) Overexpression of PIP2; 5 aquaporin alleviates effects of low root temperature on cell hydraulic conductivity and growth in Arabidopsis. Plant physiology 159: 479-488**
Pubmed: Author and Title
Google Scholar: Author Only Title Only Author and Title

**Ma F, Peterson CA (2001) Frequencies of plasmodesmata in Allium cepa L. roots: implications for solute transport pathways. Journal of Experimental Botany 52: 1051-1061**
Pubmed: Author and Title
Google Scholar: Author Only Title Only Author and Title

**Maurel C, Boursiac Y, Luu D-T, Santoni V, Shahzad Z, Verdoucq L (2015) Aquaporins in plants. Physiological reviews 95: 1321-1358**
Pubmed: Author and Title
Google Scholar: Author Only Title Only Author and Title

**Maurel C, Verdoucq L, Rodrigues O (2016) Aquaporins and plant transpiration. Plant, cell & environment 39: 2580-2587**
Pubmed: Author and Title
Google Scholar: Author Only Title Only Author and Title

**McCarty DR, Mark Settles A, Suzuki M, Tan BC, Latshaw S, Porch T, Robin K, Baier J, Avigne W, Lai J (2005) Steady-state transposon mutagenesis in inbred maize. The Plant Journal 44: 52-61**
Pubmed: Author and Title
Google Scholar: Author Only Title Only Author and Title

**McCarty DR, Suzuki M, Hunter C, Collins J, Avigne WT, Koch KE (2013) Genetic and molecular analyses of UniformMu transposon insertion lines. In Plant Transposable Elements. Springer, pp 157-166**
Pubmed: Author and Title
Google Scholar: Author Only Title Only Author and Title

**Morsomme P, de Kerchove d'Exaerde A, De Meester S, Thines D, Goffeau A, Boutry M (1996) Single point mutations in various domains of a plant plasma membrane H (+)-ATPase expressed in Saccharomyces cerevisiae increase H (+)-pumping and permit yeast growth at low pH. The EMBO Journal 15: 5513-5526**
Pubmed: Author and Title
Google Scholar: Author Only Title Only Author and Title

**Moshelion M, Moran N, Chaumont F (2004) Dynamic changes in the osmotic water permeability of protoplast plasma membrane. Plant Physiology 135: 2301-2317**
Pubmed: Author and Title
Google Scholar: Author Only Title Only Author and Title

**Nelissen H, Rymen B, Jikumaru Y, Demuynck K, Van Lijsebettens M, Kamiya Y, Inzé D, Beemster GT (2012) A local maximum in gibberellin levels regulates maize leaf growth by spatial control of cell division. Current Biology 22: 1183-1187**
Pubmed: Author and Title
Google Scholar: Author Only Title Only Author and Title

**Nelissen H, Sun XH, Rymen B, Jikumaru Y, Kojima M, Takebayashi Y, Abbeloos R, Demuynck K, Storme V, Vuylsteke M (2018) The reduction in maize leaf growth under mild drought affects the transition between cell division and cell expansion and cannot be restored by elevated gibberellic acid levels. Plant Biotechnology Journal 16: 615-627**
Pubmed: Author and Title
Google Scholar: Author Only Title Only Author and Title

**Nour-Eldin HH, Hansen BG, Nørholm MH, Jensen JK, Halkier BA (2006) Advancing uracil-excision based cloning towards an ideal technique for cloning PCR fragments. Nucleic Acids Research 34: e122-e122**
Pubmed: Author and Title
Google Scholar: Author Only Title Only Author and Title

**Parent B, Hachez C, Redondo E, Simonneau T, Chaumont F, Tardieu F (2009) Drought and abscisic acid effects on aquaporin content translate into changes in hydraulic conductivity and leaf growth rate: a trans-scale approach. Plant Physiology 149: 2000-2012**
Pubmed: Author and Title
Google Scholar: Author Only Title Only Author and Title

**Parent B, Turc O, Gibon Y, Stitt M, Tardieu F (2010) Modelling temperature-compensated physiological rates, based on the co-ordination of responses to temperature of developmental processes. Journal of Experimental Botany 61: 2057-2069**
Pubmed: Author and Title
Google Scholar: Author Only Title Only Author and Title

**Péret B, Li G, Zhao J, Band LR, Voß U, Postaire O, Luu D-T, Da Ines O, Casimiro I, Lucas M (2012) Auxin regulates aquaporin function to facilitate lateral root emergence. Nature cell biology 14: 991**
Pubmed: Author and Title
Google Scholar: Author Only Title Only Author and Title

**Postaire O, Tournaire-Roux C, Grondin A, Boursiac Y, Morillon R, Schaffner AR, Maurel C (2010) A PIP1 Aquaporin Contributes to Hydrostatic Pressure-Induced Water Transport in Both the Root and Rosette of Arabidopsis. Plant Physiology 152: 1418-1430**
Pubmed: Author and Title
Google Scholar: Author Only Title Only Author and Title

**Prado K, Maurel C (2013) Regulation of leaf hydraulics: from molecular to whole plant levels. Frontiers in plant science 4**
Pubmed: Author and Title
Google Scholar: Author Only Title Only Author and Title

**Rodrigues O, Reshetnyak G, Grondin A, Saijo Y, Leonhardt N, Maurel C, Verdoucq L (2017) Aquaporins facilitate hydrogen peroxide entry into guard cells to mediate ABA-and pathogen-triggered stomatal closure. Proceedings of the National Academy of Sciences 114: 9200-9205**
Pubmed: Author and Title
Google Scholar: Author Only Title Only Author and Title

**Sack L, Holbrook NM (2006) Leaf hydraulics. Annu. Rev. Plant Biol. 57: 361-381**
Pubmed: Author and Title
Google Scholar: Author Only Title Only Author and Title

**Sade N, Gebretsadik M, Seligmann R, Schwartz A, Wallach R, Moshelion M (2010) The role of tobacco Aquaporin1 in improving water use efficiency, hydraulic conductivity, and yield production under salt stress. Plant Physiology 152: 245-254**
Pubmed: Author and Title
Google Scholar: Author Only Title Only Author and Title

**Sade N, Shatil-Cohen A, Attia Z, Maurel C, Boursiac Y, Kelly G, Granot D, Yaaran A, Lerner S, Moshelion M (2014) The role of plasma membrane aquaporins in regulating the bundle sheath-mesophyll continuum and leaf hydraulics. Plant Physiology 166: 1609-1620**
Pubmed: Author and Title
Google Scholar: Author Only Title Only Author and Title

**Sadok W, Naudin P, Boussuge B, Muller B, Welcker C, Tardieu F (2007) Leaf growth rate per unit thermal time follows QTL-dependent daily patterns in hundreds of maize lines under naturally fluctuating conditions. Plant, Cell & Environment 30: 135-146**
Pubmed: Author and Title
Google Scholar: Author Only Title Only Author and Title

**Shatil-Cohen A, Sibony H, Draye X, Chaumont F, Moran N, Moshelion M (2014) Measuring the osmotic water permeability coefficient (Pf) of spherical cells: isolated plant protoplasts as an example. Journal of visualized experiments: JoVE**
Pubmed: Author and Title
Google Scholar: Author Only Title Only Author and Title

**Shatil-Cohen A, Attia Z, Moshelion M (2011) Bundle-sheath cell regulation of xylem-mesophyll water transport via aquaporins under drought stress: a target of xylem-borne ABA? The Plant Journal 67: 72-80**
Pubmed: Author and Title
Google Scholar: Author Only Title Only Author and Title

**Siefritz F, Tyree MT, Lovisolo C, Schubert A, Kaldenhoff R (2002) PIP1 plasma membrane aquaporins in tobacco from cellular effects to function in plants. The Plant Cell 14: 869-876**
Pubmed: Author and Title
Google Scholar: Author Only Title Only Author and Title

**Steudle E (2000) Water uptake by plant roots: an integration of views. Plant and Soil 226: 45-56**
Pubmed: Author and Title
Google Scholar: Author Only Title Only Author and Title

**Steudle E, Peterson CA (1998) How does water get through roots? Journal of Experimental Botany 49: 775-788**
Pubmed: Author and Title
Google Scholar: Author Only Title Only Author and Title

**Tyree MT, Nardini A, Salleo S, Sack L, El Omari B (2004) The dependence of leaf hydraulic conductance on irradiance during HPFM measurements: any role for stomatal response? Journal of Experimental Botany 56: 737-744**
Pubmed: Author and Title
Google Scholar: Author Only Title Only Author and Title

**Volkov V, Fricke W, Hachez C, Moshelion M, Draye X, Chaumont F (2006) Osmotic water permeability differs between growing and non-growing barley leaf tissues. Comparative Biochemistry and Physiology a-Molecular & Integrative Physiology 143: S48-S48**
Pubmed: Author and Title
Google Scholar: Author Only Title Only Author and Title

**Wang C, Hu H, Qin X, Zeise B, Xu D, Rappel W-J, Boron WF, Schroeder JI (2016) Reconstitution of CO2 regulation of SLAC1 anion channel and function of CO2-permeable PIP2; 1 aquaporin as CARBONIC ANHYDRASE4 interactor. The Plant Cell 28: 568-582**
Pubmed: Author and Title
Google Scholar: Author Only Title Only Author and Title

**Zwieniecki MA, Thompson MV, Holbrook NM (2002) Understanding the hydraulics of porous pipes: tradeoffs between water uptake and root length utilization. Journal of Plant Growth Regulation 21: 315-323**
Pubmed: Author and Title
Google Scholar: Author Only Title Only Author and Title